3. Spillantini MG, Crowther RA, Jakes R, Hasegawa M, Goedert M (1998) alpha-Synuclein in filamentous inclusions of Lewy bodies from Parkinson's disease and dementia with lewy bodies. Proc Natl Acad Sci U S A 95: 6469–6473.
4. Polymeropoulos MH, Lavedan C, Leroy E, Ide SE, Dehejia A, et al. (1997) Mutation in the alpha-synuclein gene identified in families with Parkinson's disease. Science 276: 2045–2047.
5. Zarranz JJ, Alegre J, Gomez-Esteban JC, Lezcano E, Ros R, et al. (2004) The new mutation, E46K, of alpha-synuclein causes Parkinson and Lewy body dementia. Ann Neurol 55: 164–173.
6. Kruger R, Kuhn W, Muller T, Woitalla D, Graeber M, et al. (1998) Ala30Pro mutation in the gene encoding alpha-synuclein in Parkinson's disease. Nat Genet 18: 106–108.
7. Vivacqua G, Casini A, Vaccaro R, Fornai F, Yu S, et al. (2011) Different subcellular localization of alpha-synuclein in the C57BL/6J mouse's central nervous system by two novel monoclonal antibodies. J Chem Neuroanat 41: 97–110.
8. Withers GS, George JM, Banker GA, Clayton DF (1997) Delayed localization of synelfin (synuclein, NACP) to presynaptic terminals in cultured rat hippocampal neurons. Brain Res Dev Brain Res 99: 87–94.
9. Totterdell S, Meredith GE (2005) Localization of alpha-synuclein to identified fibers and synapses in the normal mouse brain. Neuroscience 135: 907–913.
10. Hsu LJ, Mallory M, Xia Y, Veinbergs I, Hashimoto M, et al. (1998) Expression pattern of synucleins (non-Abeta component of Alzheimer's disease amyloid precursor protein/alpha-synuclein) during murine brain development. J Neurochem 71: 338–344.
11. Petersen K, Olesen OF, Mikkelsen JD (1999) Developmental expression of alpha-synuclein in rat hippocampus and cerebral cortex. Neuroscience 91: 651–659.
12. Burre J, Sharma M, Tsetsenis T, Buchman V, Etherton MR, et al. (2010) Alpha-synuclein promotes SNARE-complex assembly in vivo and in vitro. Science 329: 1663–1667.
13. Scott D, Roy S (2012) alpha-Synuclein inhibits intersynaptic vesicle mobility and maintains recycling-pool homeostasis. J Neurosci 32: 10129–10135.
14. Masliah E, Rockenstein E, Veinbergs I, Mallory M, Hashimoto M, et al. (2000) Dopaminergic loss and inclusion body formation in alpha-synuclein mice: implications for neurodegenerative disorders. Science 287: 1265–1269.
15. Winner B, Regensburger M, Schreglmann S, Boyer L, Prots I, et al. (2012) Role of alpha-synuclein in adult neurogenesis and neuronal maturation in the dentate gyrus. J Neurosci 32: 16906–16916.
16. Gomez-Tortosa E, Sanders JL, Newell K, Hyman BT (2001) Cortical neurons expressing calcium binding proteins are spared in dementia with Lewy bodies. Acta Neuropathol 101: 36–42.
17. Volpicelli-Daley LA, Luk KC, Patel TP, Tanik SA, Riddle DM, et al. (2011) Exogenous alpha-synuclein fibrils induce Lewy body pathology leading to synaptic dysfunction and neuron death. Neuron 72: 57–71.
18. Giasson BI, Jakes R, Goedert M, Duda JE, Leight S, et al. (2000) A panel of epitope-specific antibodies detects protein domains distributed throughout human alpha-synuclein in Lewy bodies of Parkinson's disease. J Neurosci Res 59: 528–533.
19. Morita S, Miyata S (2012) Synaptic localization of growth-associated protein 43 in cultured hippocampal neurons during synaptogenesis. Cell Biochem Funct.
20. Watanabe Y, Tatebe H, Taguchi K, Endo Y, Tokuda T, et al. (2012) p62/SQSTM1-dependent autophagy of Lewy body-like alpha-synuclein inclusions. PLoS One 7: e52868.
21. Tatebe H, Watanabe Y, Kasai T, Mizuno T, Nakagawa M, et al. (2010) Extracellular neurosin degrades alpha-synuclein in cultured cells. Neurosci Res 67: 341–346.
22. Fujiwara H, Hasegawa M, Dohmae N, Kawashima A, Masliah E, et al. (2002) alpha-Synuclein is phosphorylated in synucleinopathy lesions. Nat Cell Biol 4: 160–164.
23. Murphy DD, Rueter SM, Trojanowski JQ, Lee VM (2000) Synucleins are developmentally expressed, and alpha-synuclein regulates the size of the presynaptic vesicular pool in primary hippocampal neurons. J Neurosci 20: 3214–3220.
24. Shah MM, Hammond RS, Hoffman DA (2010) Dendritic ion channel trafficking and plasticity. Trends Neurosci 33: 307–316.
25. Greger IH, Ziff EB, Penn AC (2007) Molecular determinants of AMPA receptor subunit assembly. Trends Neurosci 30: 407–416.
26. Luscher B, Keller CA (2004) Regulation of GABAA receptor trafficking, channel activity, and functional plasticity of inhibitory synapses. Pharmacol Ther 102: 195–221.
27. Sheng M, Kim E (2011) The postsynaptic organization of synapses. Cold Spring Harb Perspect Biol 3.
28. Moulder KL, Jiang X, Taylor AA, Shin W, Gillis KD, et al. (2007) Vesicle pool heterogeneity at hippocampal glutamate and GABA synapses. J Neurosci 27: 9846–9854.
29. Moulder KL, Mennerick S (2005) Reluctant vesicles contribute to the total readily releasable pool in glutamatergic hippocampal neurons. J Neurosci 25: 3842–3850.
30. Gureviciene I, Gurevicius K, Tanila H (2007) Role of alpha-synuclein in synaptic glutamate release. Neurobiol Dis 28: 83–89.
31. Liu G, Wang P, Li X, Li Y, Xu S, et al. (2013) Alpha-synuclein promotes early neurite outgrowth in cultured primary neurons. J Neural Transm.
32. Nakata Y, Yasuda T, Fukaya M, Yamamori S, Itakura M, et al. (2012) Accumulation of alpha-synuclein triggered by presynaptic dysfunction. J Neurosci 32: 17186–17196.

Increased α-synuclein levels in the cerebrospinal fluid of patients with Creutzfeldt–Jakob disease

Takashi Kasai, Takahiko Tokuda, Ryotaro Ishii, Noriko Ishigami, Yoshio Tsuboi, Masanori Nakagawa, Toshiki Mizuno & Omar M. A. El-Agnaf

Journal of Neurology
Official Journal of the European Neurological Society

ISSN 0340-5354

J Neurol
DOI 10.1007/s00415-014-7334-7

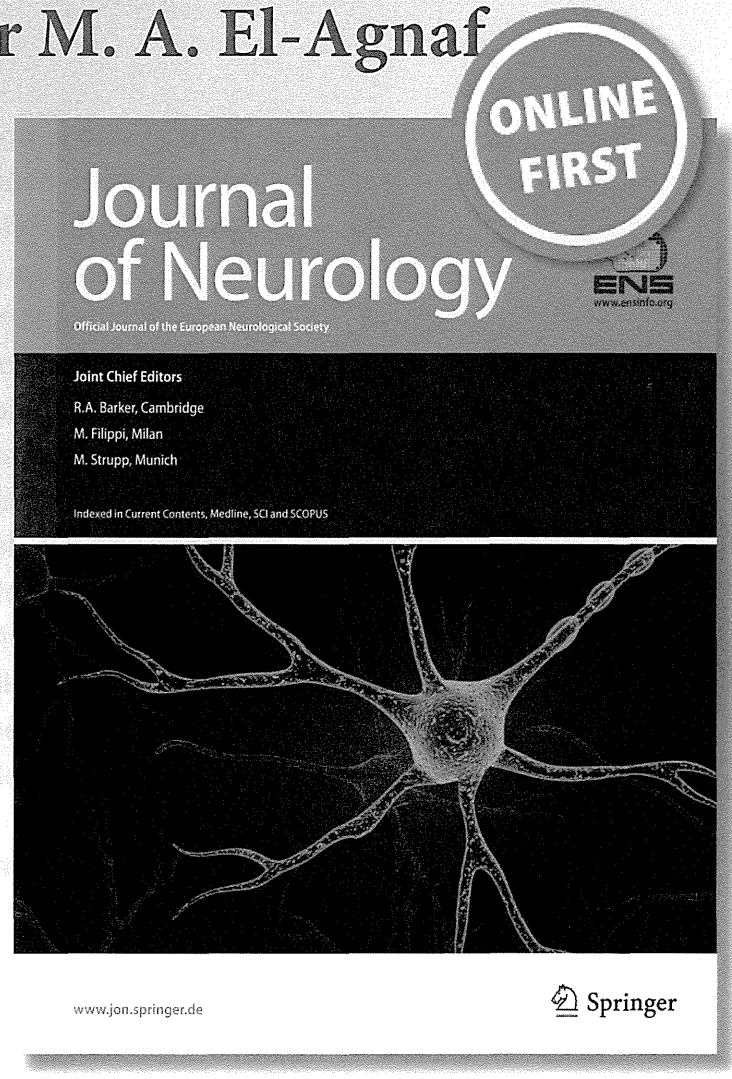

Springer

J Neurol
DOI 10.1007/s00415-014-7334-7

ORIGINAL COMMUNICATION

Increased α-synuclein levels in the cerebrospinal fluid of patients with Creutzfeldt–Jakob disease

Takashi Kasai · Takahiko Tokuda · Ryotaro Ishii · Noriko Ishigami · Yoshio Tsuboi · Masanori Nakagawa · Toshiki Mizuno · Omar M. A. El-Agnaf

Received: 13 January 2014 / Revised: 25 March 2014 / Accepted: 26 March 2014

Abstract Recent studies have shown that cerebrospinal fluid (CSF) levels of α-synuclein (α-syn) are highly elevated in patients with Creutzfeldt–Jakob disease (CJD) compared to controls. However, the diagnostic value of CSF α-syn in CJD has not been established. To confirm whether CSF α-syn is increased in CJD and is a useful marker for this disease, two independent enzyme-linked immunoabsorbent assays (ELISAs) specific for α-syn were used: ELISA 211-FL140, which is specific for full-length α-syn, and ELISA N19-FL140, which is specific for the full-length and associated C-terminal truncated forms of α-syn. CSF samples from 24 patients with CJD and 24 controls were assessed in this study. We found that samples from the CJD patients showed significantly higher levels of CSF α-syn compared to controls in both ELISA (211-FL140 or N19-FL140) tests ($P = 0.0467$ and $P = 0.0010$, respectively). However, there was a considerable overlap in the concentration ranges of the two groups of subjects. We also measured the levels of total tau (t-tau) protein in these samples and found that CSF t-tau levels were 5–10-times higher in the CJD group ($P < 0.0001$) compared with the controls. When the CSF t-tau and α-syn levels were combined, the area under the ROC curve (AUC) was slightly increased in clinically diagnosed CJD cases (AUC of 0.964) relative to an AUC of 0.943 for increased CSF t-tau alone. The combined use of CSF α-syn and t-tau levels may be a useful biomarker for the diagnosis of CJD.

Keywords Creutzfeldt–Jakob disease · Cerebrospinal fluid · α-Synuclein · Tau · Biomarker · ELISA

Introduction

Creutzfeldt–Jakob disease (CJD) is a rare neurodegenerative disease that mainly affects elderly people. The diagnosis of CJD can only be confirmed by brain biopsy; however, certain biochemical markers in cerebrospinal fluid (CSF) have been reported to be useful in the differential diagnosis of CJD from other dementia-spectrum illnesses. Several reports have demonstrated that total tau protein (t-tau) in the CSF is one of the most sensitive biomarkers in the early diagnosis of CJD [1, 2]. Tau is a microtubule-associated protein that contributes to axonal structure [3]. Therefore, axonal degeneration and the leakage of axonal proteins in the brains of CJD patients are the most likely causes of an increase in CSF levels of t-tau. However, the primary neuropathological feature in prion diseases is the loss of synapses rather than axonal degeneration [4–6], and proteins leaking from synaptic structures probably have a greater early diagnostic value than t-tau or other axonal proteins in CJD. Therefore, we investigated

Electronic supplementary material The online version of this article (doi:10.1007/s00415-014-7334-7) contains supplementary material, which is available to authorized users.

T. Kasai (✉) · T. Tokuda · R. Ishii · N. Ishigami · M. Nakagawa · T. Mizuno
Department of Neurology, Research Institute for Geriatrics, Kyoto Prefectural University of Medicine, Kyoto 602-0841, Japan
e-mail: kasaita@koto.kpu-m.ac.jp

Y. Tsuboi
Department of Neurology, Fukuoka University School of Medicine, Fukuoka 814-0180, Japan

O. M. A. El-Agnaf
Department of Biochemistry, Faculty of Medicine and Health Sciences, United Arab Emirates University, Al Ain, United Arab Emirates

Published online: 16 April 2014

the levels of the synaptic protein α-synuclein (α-syn) in CSF from patients with CJD and healthy matched controls.

α-Syn is a protein involved in the pathogenesis of Parkinson's disease (PD) and other synucleinopathies. Recently, our group and others have developed protocols for sandwich-type enzyme-linked immunoabsorbent assays (ELISAs) specific for α-syn and have reported decreased CSF levels of α-syn in patients with PD compared to controls [7–10]. Interestingly, it has been reported that CSF levels of α-syn were highly elevated in eight CJD patients compared with controls [9]. The strong increase in the CSF levels of α-syn in CJD patients was interpreted as biochemical evidence of rapid synaptic degeneration and leakage of α-syn, which is known to be a major component of presynaptic proteins [11], in CJD. Although it has been implied that CSF α-syn could be a diagnostic marker for CJD, relatively few patients have been studied, and thus study size has been insufficient for evaluating the diagnostic value. To verify these previous findings and to evaluate the diagnostic utility of CSF α-syn for CJD, we investigated the levels of α-syn in CSF from 24 patients with CJD and 24 control subjects.

Methods and materials

Patients

CSF samples were collected from 24 patients with CJD (age 41–82, mean ± SD = 62.9 ± 10.0) and 24 gender- and age-matched control subjects (age 17–88, mean ± SD = 60.0 ± 18.3). The CJD group included two patients with familial CJD (V180I), three patients with probable iatrogenic CJD (iCJD) and 19 patients with probable sporadic CJD (sCJD). Probable sCJD and iCJD patients fulfilled the WHO diagnostic criteria for CJD [12]. The control group included neurologically normal individuals ($n = 8$) as well as subjects with peripheral neuropathy ($n = 8$), cranial neuropathy ($n = 3$), epilepsy ($n = 2$), motor neuron disease ($n = 1$), spastic paraplegia ($n = 1$), and spinal myoclonus ($n = 1$). Informed consent was obtained from the patient when possible or from the nearest relative when not possible, which was approved by the University Ethics Committee (Kyoto Prefectural University of Medicine, Kyoto, and the Fukuoka University School of Medicine, Fukuoka, Japan). The study procedures were designed and performed in accordance with the Declaration of Helsinki. Fresh CSF samples collected from living CJD patients and control cases were cleared by centrifugation at 3,000×g for 10 min at 4 °C and then stored at −80 °C until used for this study. We excluded samples with apparent blood contamination from this study following visual inspection of centrifuged CSF. Samples with pink-red discoloration indicative of hemoglobinemia were excluded.

Antibodies

The anti-human α-syn monoclonal antibody 211 (MAb211) recognizes the C-terminal portion of α-syn (residues 121–125). The anti-human α-/β-synuclein goat polyclonal antibody N19 recognizes the N-terminal portion of α-syn (residues 5–19). The anti-human α-/β-/γ-synuclein rabbit polyclonal antibody FL-140 was raised against the recombinant full-length α-syn (Fig. 1a). All antibodies were purchased from Santa Cruz Biotechnology, CA, USA.

Measurement of α-syn

CSF α-syn levels were measured using a previously reported sandwich ELISA system that was modified to achieve an improved sensitivity as low as 0.01 pg/ml [7]. Briefly, each ELISA plate (384-well ELISA plate, Nunc Maxisorb™, NUNC A/S, Roskilde, Denmark) was coated with 1 μg/ml of either MAb211 or N19 antibodies (50 μl/well) as a capture antibody in 200 mM $NaHCO_3$, pH 9.6, at 4 °C for overnight. The plate was then washed with phosphate buffered saline (PBS) containing 0.05 % Tween 20 (PBST) and subsequently incubated with 100 μl/well of a blocking buffer (PBST containing 2.5 % gelatin) for 2 h at 37 °C. After adding a cocktail of protease inhibitors (Calbiochem, CA, USA) to the CSF samples, 50 μl of these samples were added to each well and the plate was incubated at 37 °C for 3 h. After washing with PBST, 50 μl of anti-α-syn antibody FL-140 (0.2 mg/ml in the blocking buffer) was added as a reporter antibody, and the plate was incubated at 37 °C for 2 h. After washing with PBST, the wells were incubated with 50 μl/well of horseradish peroxidase (HRP)-labeled anti-rabbit immunoglobulins (DAKO, Glostrup, Denmark) and incubated for 1 h at 37°C. Bound HRP activity was assayed using an enhanced chemiluminescent substrate (SuperSignal Femto Maximum Sensitivity Substrate, Pierce Biotechnology, Rockford, IL, USA, 50 μl/well), and the chemiluminescence signal was measured at 395 nm with a microplate luminometer (SpectraMax L, Molecular Devices, Tokyo, Japan). The standard curve for the ELISA was prepared using 50 μl/well of recombinant human α-syn solution at different concentrations of the protein in PBS solution. All samples and standards were run in triplicate on the same day with the same lot of standards unless otherwise noted. The relative estimated concentrations of CSF α-syn were calculated using a standard curve. In the following descriptions, the use of MAb211 as the capture antibody and FL140 as the reporter antibody is referred to as "211-FL140 ELISA", and the use of N19 as the capture antibody and

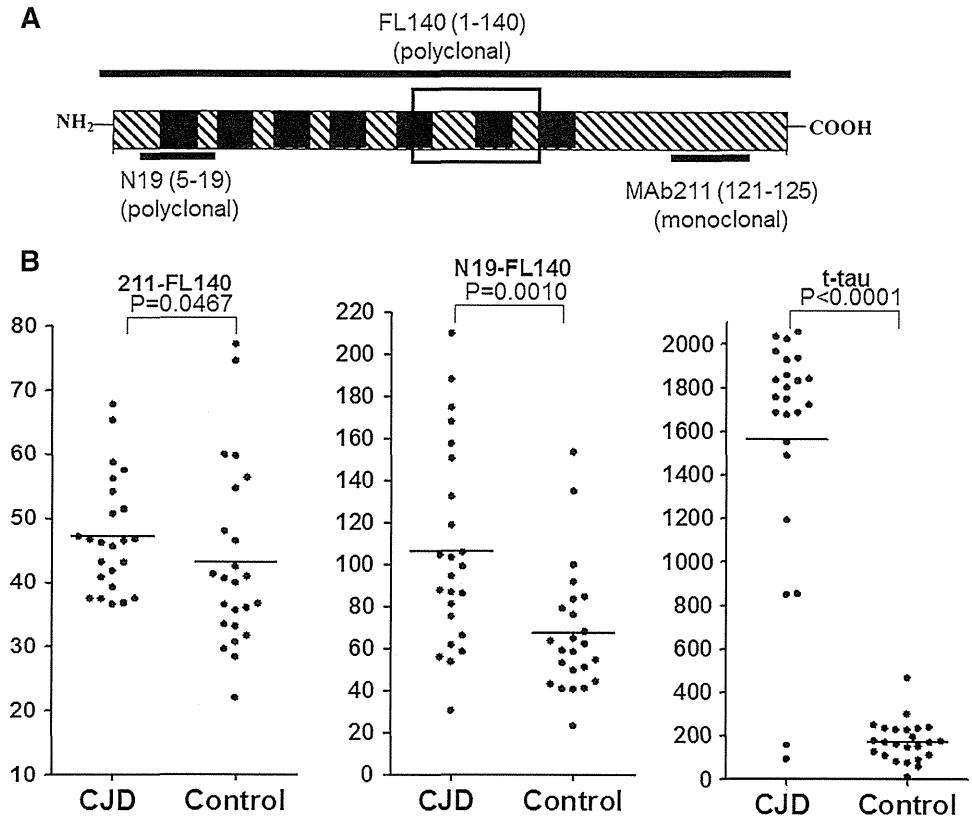

Fig. 1 **a** Recognition sequences for α-syn antibodies. Recognition sequences for α-syn antibodies used in the present study are shown as *black bars* in the schema of the primary structure of α-syn. *Black boxes* indicate imperfect lysine-rich motifs (KTKEGV), and the *white box* indicates the non-amyloid-β component (NAC) domain. **b** Scatter plots of the levels of CSF α-syn, measured using 211-FL140 ELISA and N19-FL140 ELISA, and the levels of t-tau. The CSF α-syn concentrations measured with two ELISA methods, 211-FL140 ELISA, N19-FL140 ELISA, and the t-tau levels measured using a commercial kit are shown. The concentrations of CSF α-syn in the CJD group were significantly higher than that in the age-matched control subjects for either ELISA ($P = 0.0467$ using 211-FL140 ELISA, and $P = 0.0010$ using N19-FL140 ELISA, Mann–Whitney U test). The levels of t-tau were highly elevated in the CJD group ($P < 0.0001$, Mann–Whitney U test)

FL140 as the reporter antibody is referred to as "N19-FL140 ELISA". The 211-FL140 ELISA is specific for the full-length human α-syn because of the selective affinity of MAb211 for α-syn. In contrast, N19 recognizes the N-terminal sequence of α-syn, which is shared by β-synuclein (β-syn) (Fig. 1a); therefore, N19-FL140 ELISA can detect both proteins. However, using mass spectroscopy, we have reported that neither β-syn nor γ-synuclein was detected in human CSF [9], and therefore, our N19-FL140 ELISA array only measures the α-syn present in CSF. It is noteworthy that this ELISA protocol can also detect the C-terminal truncated forms of α-syn present in CSF, which cannot be detected by the 211-FL140 ELISA protocol.

Measurement of t-tau

The levels of CSF t-tau were measured using the Fino Scholar hTau ELISA kit (Nipro, Osaka, Japan) according to the manufacturer's instructions.

Statistics

Image analysis was performed using Scion Image for Windows Version 4 (Scion Corporation Frederick, MA, USA). A comparison between the two independent groups was performed using the Mann–Whitney U test. The ROC curve and the AUC were calculated and compared between the two α-syn ELISA arrays. $P < 0.05$ was considered statically significant. Statistical analyses were performed using GraphPad Prism Version 4.0 (GraphPad Software, San Diego, CA, USA).

Results

As shown in Fig. 1b, the concentrations of CSF α-syn measured using the 211-FL140 ELISA were significantly higher in CJD patients than in controls (mean ± SD; 47.28 ± 8.98 in CJD vs. 42.33 ± 12.53 in controls,

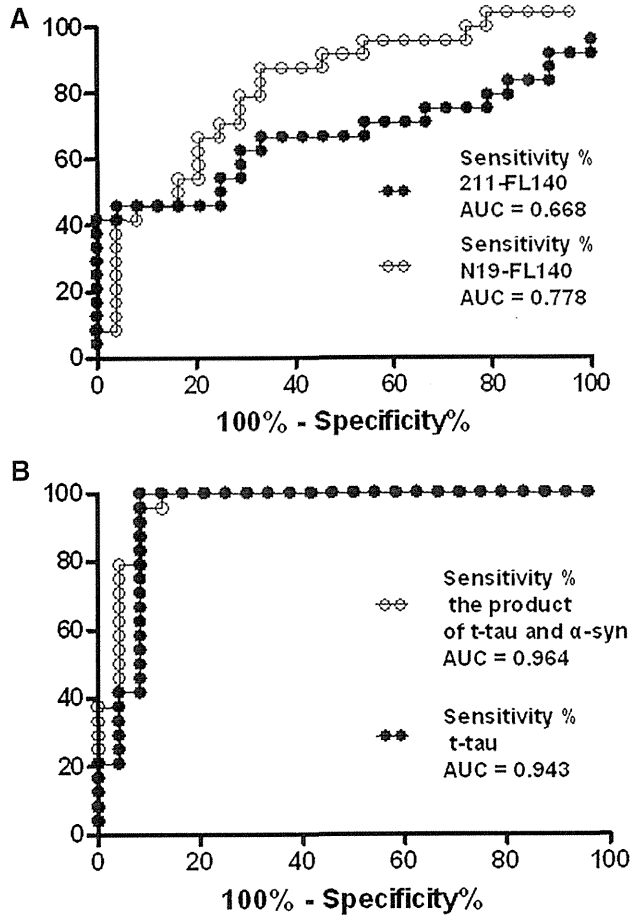

Fig. 2 **a** Receiver operating characteristic (ROC) curves for the levels of α-syn in CSF in the discrimination of patients with CJD from controls when using the 211-FL140 ELISA (*black circles*) and the N19-FL140 ELISA (*white circles*). AUC values are indicated. **b** ROC curves for the use of t-tau alone (*black circles*) and the use of combined t-tau and α-syn (*white circles*) in the discrimination of patients with CJD from controls. AUC values are indicated

$P = 0.0467$). However, there was a considerable overlap in the concentration ranges for the two groups. Receiver operating characteristic (ROC) curves used to discriminate patients with CJD from the control subjects were calculated based on ELISA data. The area under the ROC curve (AUC) for the 211-FL140 ELISA was poor (AUC = 0.668) (Fig. 2a). Using the N19-FL140 ELISA, significantly higher levels of CSF α-syn were detected in CJD patients than in controls (mean ± SD; 106.3 ± 47.23 in CJD vs. 66.38 ± 26.76 in controls, $P = 0.0010$). The AUC in the ROC curve used to discriminate CJD patients from controls improved in the N19-FL140 ELISA (AUC = 0.778) (Fig. 2a), although an overlap in the concentration ranges for the two groups was still observed, and the mean value of the signals in the CJD group was no more than twice that of the control group.

We also measured the levels of total tau (t-tau) in CJD and control samples. The mean value of t-tau in controls corresponded with previously reported levels (mean ± SD; 188 ± 103 pg/ml) [13].The CSF levels of t-Tau were highly elevated in the CJD group ($P < 0.0001$, Mann–Whitney U test) with mean values 5–10-times higher than in control patients (mean ± SD; 1,564.11 ± 548.16 pg/ml in CJD vs. 173.77 ± 93.57 pg/ml in controls). However, two CJD patients who had normal levels of CSF t-tau also had elevated levels of CSF α-syn, as measured with the N19-FL140 ELISA (87.8 and 105.8 ng/ml), that exceeded the threshold value of 77.7 ng/ml. The measured levels of CSF t-tau and α-syn in CJD patients are summarized in Table 1. When we calculated the values of t-tau and α-syn measured with the N19-FL140 ELISA, the AUC of the product (0.964) was slightly higher than that of t-tau alone (0.943) in the ROC analysis (Fig. 2b). The optimized threshold value of the product was 14,922 ng/ml, where the sensitivity and specificity of the test were 79.17 and 95.83 %, respectively.

Discussion

The CSF levels of α-syn measured with the 211-FL140 ELISA were significantly higher in CJD patients than in controls. Our data is in agreement with the results reported by Mollenhauer et al. [9]. In this earlier report, CSF α-syn levels in CJD were more than 40 times higher than in controls [9], whereas our results recorded a sizeable overlap between the concentration ranges for individual signals for CJD patients and controls. Such a discrepancy could be caused by the narrow binding specificity of MAb211, which only binds to the full-length α-syn [14]; thus, an alternative assay system (N19-FL140 ELISA) was developed in which full-length α-syn and its C-terminal truncated forms are detectable. Interestingly, the N19-FL140 assay showed better diagnostic performance than did the 211-FL140 assay. However, the large signal difference between the CJD patients and the control group reported by Mollenhauer and co-workers [9] was not reproduced in our current study. Such inconsistencies among different studies may be caused by methodological issues, including pre-analytical differences in the collection, handling, and storage of CSF samples as well as the use of antibodies that detect different species of α-syn. In fact, when we performed immunoprecipitation followed by western blotting as an alternative approach to roughly estimate the CSF α-syn levels detected with ELISA, we found that the density of the band for full-length α-syn in CJD patients was much higher than that in controls in IP-WB (Supplementary Figure). We currently have no clear

Table 1 Concentrations of CSF t-tau and α-syn measured in CJD patients

Patient No.	Sex	Age	CJD type	*PRNP* codon 129 genotyope	*PRNP* codon 219 genotyope	α-Syn (ng/ml) measured using 211-FL140 ELISA	α-/β-Syn (ng/ml) measured using N19-FL140 ELISA	t-Tau (pg/ml)
1	M	60	sCJD	ND	ND	39.25	30.48	852.03
2	M	72	sCJD	ND	ND	67.74	118.89	1,799.73
3	M	41	sCJD	ND	ND	56.19	75.33	1,719.62
4	M	54	sCJD	MM	EE	57.50	174.89	1,830.18
5	*F*	*49*	*iCJD*	*MM*	*EE*	*51.45*	*87.77*	*91.72*
6	F	59	sCJD	ND	ND	54.16	86.23	1,833.75
7	F	61	sCJD	MM	EE	45.64	56.04	1,684.48
8	F	68	sCJD	MM	EE	47.14	94.45	1,965.74
9	F	68	sCJD	ND	ND	37.48	61.78	1,934.51
10	F	82	sCJD	ND	ND	46.48	99.11	1,684.72
11	F	64	sCJD	ND	ND	41.81	157.69	847.09
12	F	49	sCJD	MM	EE	46.69	58.57	1,745.42
13	*F*	*69*	*sCJD*	*MM*	*EE*	*46.75*	*105.84*	*156.77*
14	F	60	sCJD	MM	EE	40.76	81.18	1,755.35
15	F	60	fCJD (V180I)	MM	EE	65.31	86.77	1,674.99
16	F	55	sCJD	MM	EE	50.74	132.49	2,034.30
17	F	68	sCJD	MM	EE	58.73	103.30	2,021.94
18	M	50	iCJD	ND	ND	36.79	66.11	1,191.23
19	M	62	iCJD	MM	EE	43.11	210.13	1,488.26
20	F	69	fCJD (V180I)	MM	EE	37.49	150.74	1,550.17
21	F	79	sCJD	MM	EE	43.19	188.22	1,926.43
22	F	65	sCJD	MM	EE	36.58	168.03	1,839.54
23	M	73	sCJD	ND	ND	37.43	104.62	1,855.61
24	F	73	sCJD	ND	ND	46.20	53.69	2,054.96
					Mean	47.27	106.35	1,564.11
					SD	8.91	47.23	548.16

Some cases did not agree to allow genetic testing. The *PRNP* genotypes of these patients are presented as ND (not determined). Two CJD patients had normal CSF t-tau levels (indicated by italic) and high CSF α-syn levels of as measured with the N19-FL140 ELISA

sCJD sporadic CJD, *fCJD* familial CJD, *iCJD* iatrogenic CJD

explanation for this discrepancy between our ELISA and IP-WB. However, this result suggests that detection by our ELISA of unknown α-syn species that leaked out into the CSF space in CJD patients still requires improvement. It cannot be said that the diagnostic value of the ELISA tests studied here for measuring CSF α-syn in CJD exceeds that of the conventional biomarker, t-tau. However, a few CJD patients in the present study with normal levels of t-tau showed elevated CSF α-syn levels (see Tables 1 and 2). Signal overlap is often seen in cross-sectional investigations, such as in the quantification of CSF Aβ and tau proteins as biomarkers for Alzheimer's disease [15]. In clinical practice, it has been documented that the predictive value of CSF parameters in individual subjects is often enhanced by employing more than one surrogate or biomarker. Accordingly, the combined CSF t-tau and α-syn results improved the ability to discriminate between the CJD patients and controls compared with the use of CSF t-tau alone (see Fig. 2b). The AUC value, which represents the ability to discriminate between CJD patients and controls, was 0.943 for CSF t-tau alone but was slightly increased to 0.964 by combining CSF t-tau with α-syn, implying that the CSF α-syn species measured by the N19-FL140 ELISA may be a complementary biomarker to t-tau for the diagnosis of CJD.

A potential confounder in this study is the imperfect exclusion of samples contaminated with blood. Hong et al. [8] indicated that samples contaminated by red blood cells, which are a potential source of α-syn, should be excluded using hemoglobin measures. On the other hand, not all ELISAs detect α-syn that has leaked from red blood cells. Fould et al. reported that CSF α-syn levels from four independent ELISAs, including the 211-FL140 ELISA that we used, do not correlate with hemoglobin concentrations. Therefore, she argued that these ELISAs are applicable for

Table 2 Concentrations of CSF t-tau and α-syn measured in control subjects

Patient No.	Sex	Age	Diseases	α-Syn (ng/ml) measured using 211-FL140 ELISA	α-/β-Syn (ng/ml) measured using N19-FL140 ELISA	t-Tau (pg/ml)
1	F	66	Neuropathy	33.13	51.24	80.93
2	M	64	Neuropathy	74.53	135.05	160.77
3	M	58	Neuropathy	30.69	40.52	150.67
4	M	75	Normal	39.96	54.72	225.73
5	M	72	Epilepsy	33.44	40.90	174.11
6	F	21	Epilepsy	46.52	63.73	169.48
7	F	47	MND	40.62	44.42	298.34
8	F	39	Normal	31.69	41.21	176.34
9	M	38	Spastic paraplegia	48.01	68.09	126.03
10	F	59	Neuropathy	22.00	23.22	239.02
11	F	48	Normal	59.77	83.54	248.84
12	M	17	Neuropathy	41.27	58.60	193.30
13	M	40	Normal	56.35	91.90	233.68
14	F	71	Normal	54.65	99.93	110.62
15	M	73	Normal	59.93	84.82	146.76
16	M	67	Spinal myoclonus	42.48	79.14	107.41
17	F	63	Neuropathy	77.16	153.71	234.33
18	F	76	Cranial neuropathy	28.37	53.15	228.10
19	F	60	Neuropathy	36.51	59.06	9.34
20	M	77	Normal	40.95	76.21	75.84
21	M	75	Neuropathy	35.63	49.65	169.41
22	M	88	Normal	29.62	43.10	464.68
23	F	69	Cranial neuropathy	36.05	62.25	88.90
24	M	78	Cranial neuropathy	36.70	64.85	57.79
			Mean	43.17	67.62	173.77
			SD	14.12	30.06	93.57

We found no significant difference in any parameter between the normal controls and the other neurological disease controls ($P = 0.327$ for α-syn measured using 211-FL140 ELISA, $P = 0.270$ for α-/β-syn measured using N19-FL140 ELISA, and $P = 0.327$ for t-tau)

MND motor neuron disease

CSF that may be contaminated with small amounts of blood, such as post-mortem CSF [16]. The cause of such inconsistency among reports is still unclear. Regarding the ELISA that we used in this study, we have also confirmed that no correlation exists between levels of hemoglobin and α-syn in CSF (unpublished data).

In summary, the present study found that CSF α-syn levels in patients with CJD were significantly higher than in controls when we used an ELISA protocol specific for detecting only the full-length α-syn. This result was consistently verified with an additional ELISA protocol that detects not only the full-length form but also the C-terminal truncated forms of α-syn. Although these observations were consistent with previously reported results, the large signal difference between the groups that has been previously reported was not observed in the present report. In this study, we demonstrated that the diagnostic value of CSF α-syn alone does not exceed that of CSF t-tau; however, the AUC value was slightly increased when we combined the use of both markers.

Acknowledgments This work was supported by Grants-in-Aid from the Research Committee of CNS Degenerative Disease, the Ministry of Health, Labor, and Welfare of Japan (to T.T.), and Grants-in-Aid (No. 23591252 to T.T. and No. 21790847 to T.K.) from the Ministry of Education, Culture, Sports, Science and Technology of Japan. The laboratory of Omar M. El-Agnaf is supported by the Michael J. Fox Foundation for Parkinson's Research (NY, USA).

Conflicts of interest All authors have no conflict of interest to declare.

Ethical standard All human studies must state that they have been approved by the appropriate ethics committee and have therefore been performed in accordance with the ethical standards laid down in the 1964 Declaration of Helsinki.

References

1. Satoh K, Shirabe S, Tsujino A, Eguchi H, Motomura M, Honda H, Tomita I, Satoh A, Tsujihata M, Matsuo H, Nakagawa M, Eguchi K (2007) Total tau protein in cerebrospinal fluid and diffusion-weighted MRI as an early diagnostic marker for Creutzfeldt–Jakob disease. Dement Geriatr Cogn Disord 24:207–212

2. Hamlin C, Puoti G, Berri S, Sting E, Harris C, Cohen M, Spear C, Bizzi A, Debanne SM, Rowland DY (2012) A comparison of tau and 14-3-3 protein in the diagnosis of Creutzfeldt–Jakob disease. Neurology 79:547–552. doi:10.1212/WNL.0b013e318263565f
3. Goedert M, Crowther RA, Garner CC (1991) Molecular characterization of microtubule-associated proteins tau and MAP2. Trends Neurosci 14:193–199
4. Fournier JG (2008) Cellular prion protein electron microscopy: attempts/limits and clues to a synaptic trait. Implications in neurodegeneration process. Cell Tissue Res 332:1–11. doi:10.1007/s00441-007-0565-5
5. Clinton J, Forsyth C, Royston MC, Roberts GW (1993) Synaptic degeneration is the primary neuropathological feature in prion disease: a preliminary study. Neuroreport 4:65–68
6. Jeffrey M, Halliday WG, Bell J, Johnston AR, MacLeod NK, Ingham C, Sayers AR, Brown DA, Fraser JR (2000) Synapse loss associated with abnormal PrP precedes neuronal degeneration in the scrapie-infected murine hippocampus. Neuropathol Appl Neurobiol 26:41–54
7. Tokuda T, Salem SA, Allsop D, Mizuno T, Nakagawa M, Qureshi MM, Locascio JJ, Schlossmacher MG, El-Agnaf OM (2006) Decreased α-synuclein in cerebrospinal fluid of aged individuals and subjects with Parkinson's disease. Biochem Biophys Res Commun 349:162–166
8. Hong Z, Shi M, Chung KA, Quinn JF, Peskind ER, Galasko D, Jankovic J, Zabetian CP, Leverenz JB, Baird G, Montine TJ, Hancock AM, Hwang H, Pan C, Bradner J, Kang UJ, Jensen PH, Zhang J (2010) DJ-1 and α-synuclein in human cerebrospinal fluid as biomarkers of Parkinson's disease. Brain 133:713–726. doi:10.1093/brain/awq008
9. Mollenhauer B, Cullen V, Kahn I, Krastins B, Outeiro TF, Pepivani I, Ng J, Schulz-Schaeffer W, Kretzschmar HA, McLean PJ, Trenkwalder C, Sarracino DA, Vonsattel JP, Locascio JJ, El-Agnaf OM, Schlossmacher MG (2008) Direct quantification of CSF α-synuclein by ELISA and first cross-sectional study in patients with neurodegeneration. Exp Neurol 213:315–325. doi:10.1016/j.expneurol.2008.06.004
10. Mollenhauer B, Locascio JJ, Schulz-Schaeffer W, Sixel-Doring F, Trenkwalder C, Schlossmacher MG (2011) α-Synuclein and tau concentrations in cerebrospinal fluid of patients presenting with parkinsonism: a cohort study. Lancet Neurol 10:230–240. doi:10.1016/S1474-4422(11)70014-X
11. Beyer K (2007) Mechanistic aspects of Parkinson's disease: α-synuclein and the biomembrane. Cell Biochem Biophys 47:285–299
12. Zeidler M, Gibbs CJ Jr, Meslin F (1998) WHO mannual for strengthening diagnosis and surveillance of Creuzfeldt-Jakob disease. World Health Organization, Geneva, pp 47–51
13. Nishimura T, Takeda M, Nakamura Y, Yosbida Y, Arai H, Sasaki H, Shouji M, Hirai S, Khise K, Tanaka K, Hamamoto M, Yamamoto H, Matsubayashi T, Urakami K, Adachi Y, Nakashima K, Toji H, Nakamura S, Yoshida H (1998) Basic and clinical studies on the measurement of tau protein in cerebrospinal fluid as a biological marker for Alzheimer's disease and related disorders: multicenter study in Japan. Methods Find Exp Clin Pharmacol 20:227–235
14. El-Agnaf OM, Salem SA, Paleologou KE, Cooper LJ, Fullwood NJ, Gibson MJ, Curran MD, Court JA, Mann DM, Ikeda S, Cookson MR, Hardy J, Allsop D (2003) α-Synuclein implicated in Parkinson's disease is present in extracellular biological fluids, including human plasma. FASEB J 17:1945–1947
15. Motter R, Vigo-Pelfrey C, Kholodenko D, Barbour R, Johnson-Wood K, Galasko D, Chang L, Miller B, Clark C, Green R et al (1995) Reduction of beta-amyloid peptide42 in the cerebrospinal fluid of patients with Alzheimer's disease. Ann Neurol 38:643–648
16. Foulds PG, Yokota O, Thurston A, Davidson Y, Ahmed Z, Holton J, Thompson JC, Akiyama H, Arai T, Hasegawa M, Gerhard A, Allsop D, Mann DM (2012) Post mortem cerebrospinal fluid α-synuclein levels are raised in multiple system atrophy and distinguish this from the other α-synucleinopathies, Parkinson's disease and Dementia with Lewy bodies. Neurobiol Dis 45:188–195. doi:10.1016/j.nbd.2011.08.003

Neurobiology of Disease 73 (2015) 244–253

Contents lists available at ScienceDirect

Neurobiology of Disease

journal homepage: www.elsevier.com/locate/ynbdi

Lysosomal enzyme cathepsin B enhances the aggregate forming activity of exogenous α-synuclein fibrils

Atsushi Tsujimura [a], Katsutoshi Taguchi [a], Yoshihisa Watanabe [a], Harutsugu Tatebe [b], Takahiko Tokuda [b], Toshiki Mizuno [b], Masaki Tanaka [a,*]

[a] Department of Basic Geriatrics, Kyoto Prefectural University of Medicine, Kawaramachi-Hirokoji, Kamikyo-ku, Kyoto 602-8566, Japan
[b] Department of Neurology, Kyoto Prefectural University of Medicine, Kawaramachi-Hirokoji, Kamikyo-ku, Kyoto 602-8566, Japan

ARTICLE INFO

Article history:
Received 30 July 2014
Revised 1 October 2014
Accepted 12 October 2014
Available online 22 October 2014

Keywords:
α-Synuclein
Fibril
Aggregate formation
Cathepsin B
Lysosome

ABSTRACT

The formation of intracellular aggregates containing α-synuclein (α-Syn) is one of the key steps in the progression of Parkinson's disease and dementia with Lewy bodies. Recently, it was reported that pathological α-Syn fibrils can undergo cell-to-cell transmission and form Lewy body-like aggregates. However, little is known about how they form α-Syn aggregates from fibril seeds. Here, we developed an assay to study the process of aggregate formation using fluorescent protein-tagged α-Syn-expressing cells and examined the aggregate forming activity of exogenous α-Syn fibrils. α-Syn fibril-induced formation of intracellular aggregates was suppressed by a cathepsin B specific inhibitor, but not by a cathepsin D inhibitor. α-Syn fibrils pretreated with cathepsin B *in vitro* enhanced seeding activity in cells. Knockdown of cathepsin B also reduced fibril-induced aggregate formation. Moreover, using LAMP-1 immunocytochemistry and live-cell imaging, we observed that these aggregates initially occurred in the lysosome. They then rapidly grew larger and moved outside the boundary of the lysosome within one day. These results suggest that the lysosomal protease cathepsin B is involved in triggering intracellular aggregate formation by α-Syn fibrils.

Introduction

Alpha-synuclein (α-Syn) is a major component of Lewy bodies (LBs), which are the intracellular pathological inclusions seen in synucleinopathies such as Parkinson's disease (PD), and dementia with Lewy bodies (DLB). α-Syn oligomers/fibrils are considered to underlie the disturbances of a number of intracellular processes including mitochondrial functions (Protter et al., 2012) and protein degradation processes (Xilouri et al., 2013), which may finally induce neuronal death. Studies using the brains of patients with PD have indicated that LB and Lewy neurite pathologies occur first in a few specific regions of the lower brain stem and olfactory bulb, and then spread into other regions of the brain as the disease progresses (Braak et al., 2004). Furthermore, recent studies have demonstrated the ability of α-Syn fibrils to transfer between cells, both in cultured cells and in mice (Desplats et al., 2009; Emmanouilidou et al., 2010; Alvarez-Erviti et al., 2011). Thus, it is now considered that the propagation of LB pathology in the brains of PD patients is in part due to the transmission of pathogenic polymerized forms of α-Syn. Knowledge about each step of this α-Syn transfer is being accumulated; for example, it was found that pathological α-Syn oligomers or fibrils can be internalized *via* endocytic pathways (Lee et al., 2005; Sung et al., 2001). Incorporated α-Syn fibrils are preferentially processed for degradation by the autophagy–lysosomal pathway (ALP) (Watanabe et al., 2012). Some α-Syn aggregates can induce the rupture of lysosomes following their endocytosis in neuronal cell lines (Freeman et al., 2013); on the other hand, α-Syn may also be secreted *via* exosome-mediated release (Danzer et al., 2012; Marques and Outeiro, 2012). However, the process by which α-Syn undergoes nucleation-dependent accumulation into LB-like aggregates in cells has not been fully elucidated. There have been a considerable number of *in vitro* and *in vivo* studies of oligomerization/fibrillation from the unfolded α-Syn monomer (Giasson et al., 1999; Conway et al., 1998; Hashimoto et al., 1998), and of aggregate formation after the introduction of α-Syn seeds (Luk et al., 2012a,b; Sacino et al., 2013). We also recently suggested that intracellular aggregate formation induced by exogenous α-Syn fibrils is dependent on the expression level of endogenous α-Syn in hippocampal neurons (Taguchi et al., 2014). However, the initiation step in aggregation from the fibril template has not been fully investigated.

In the present study, using an α-Syn-enhanced cyan fluorescent protein (ECFP)-expressing cell line, we established a system to evaluate the seeding activity of *in vitro*-prepared α-Syn fibrils into aggregates. Using this system, we unexpectedly found that cathepsin B, which is one of the proteolytic enzymes responsible for degrading proteins in the lysosome, enhances the aggregate forming activity of α-Syn fibrils, and that intracellular α-Syn aggregates begin to appear in the lysosome.

* Corresponding author. Fax: +81 75 251 5797.
E-mail address: mtanaka@koto.kpu-m.ac.jp (M. Tanaka).
Available online on ScienceDirect (www.sciencedirect.com).

http://dx.doi.org/10.1016/j.nbd.2014.10.011
0969-9961/

Materials and methods

Chemicals and antibodies

Three α-Syn antibodies, anti-α-Syn polyclonal antibody (C20) (Santa Cruz Biotechnology, Inc. CA), anti-α-Syn monoclonal antibody (syn-1) (BD Bio Sciences, New Jersey) and anti-phosphorylated α-Syn (pSyn) antibody (Ser129) (Wako Pure Chemical Industries Ltd, Osaka, Japan) were used in this study. Anti-GFP and anti-LC3 antibodies were purchased from Medical & Biological Laboratories Co., Ltd. (Nagoya, Japan). Anti-LAMP-2 monoclonal antibody was purchased from BD Bio Sciences (New Jersey). Anti-cathepsin B antibody was purchased from Sigma-Aldrich (St Louis, MO). Sertraline was purchased from Tocris Bioscience (Bristol, UK). Protease inhibitors, pepstatin A, CA-74Me, and E-64d were purchased from Peptide Institute Inc. (Osaka, Japan), and LysoTracker Red DND-99 was purchased from Thermo Fisher Scientific Life Technologies Invitrogen (Massachusetts).

Cell culture

Cells were grown in DMEM medium supplemented with 10% fetal bovine serum. Human α-Syn cDNA was cloned into pECFP-N1 (TAKARA BIO INC., Otsu, Japan) and the resulting expression vector was transfected into HEK293F cells with Lipofectamine 2000 (Thermo Fisher Scientific, Invitrogen). After selection with 400 μg/ml G418, a clonal-derived HEK293F/Syn-ECFP cell line was used in the intracellular aggregate-forming assay.

Preparation of recombinant α-Syn and its aggregates

Human α-Syn cDNA was amplified by PCR (forward primer, 5′-ATCA TATGGATGTATTCATGAAAGG-3′; reverse primer, 5′-ACAAGCTTGGCTTC AGGCTCATAGTC-3′) and the resultant fragment was digested with NdeI and HindIII, and then cloned into NdeI-HindIII sites of the pET43.1a *E. coli* expression vector (Merck Millipore, MA). The PrimeSTAR Mutagenesis Basal Kit (Takara Bio Inc.) was used to make a α-Syn S129A point mutation according to the manufacturer's instructions using the synthetic primers S129A_FW 5′-CCTGCTGAGGAAGGGTATCAAGAC TA-3′ and Mut-Re1 5′-CATTTCATAAGCCTCATTGTCAGGATCC-3′. Recombinant α-Syn was expressed in *E. coli* strain BL21 codonPlus (DE3) (Agilent Technologies, Santa Clara, CA) with 1 mM IPTG induction and recovered by osmotic shock into buffer consisting of 25 mM Tris–HCl/1 mM EDTA, pH 8.0. The recovered periplasmic fraction was boiled for 10 min and insoluble debris was removed by centrifugation. The cleared supernatant containing recombinant α-Syn was charged on a Hitrap Q column (GE Healthcare, UK) and eluted with a 0–1 M NaCl linear gradient. Finally, the protein was desalted with disposable PD-10 Desalting Columns with PBS and stored at −20 °C.

Fibril forms of α-Syn were prepared in accordance with a previous report (Volpicelli-Daley et al., 2011). Briefly, fibrils of α-Syn were generated by incubating purified α-Syn in PBS at a final concentration of 2 mg/ml with constant agitation (500 rpm) at 37 °C for 168 h. Then, fibrils were recovered by ultracentrifugation (110,000 ×*g*, 20 min), resuspended in PBS with brief sonication and stored at −20 °C. *In vitro* protein aggregation was monitored using the ProteoStat protein aggregation assay kit (Enzo Life Sciences, Plymouth Meeting, PA) and a CytoFluor2300 system (Thermo Fisher Scientific, Applied Biosystems) equipped with excitation 530 nm and emission 590 nm filters.

Intracellular aggregate forming assay

For the assay, 1 μg or less of α-Syn monomer/oligomer/fibrils in 25 μl of DMEM medium (resuspended with brief sonication) and 1 μl of DMRIE-C transfection reagents (Thermo Fisher Scientific, Invitrogen) in 25 μl DMEM were combined and incubated for 20 min at room temperature. The complex solution was then mixed with 50 μl of trypsin-isolated HEK293F/Syn-ECFP cell suspension (1×10^5/50 μl) in 96-well plates. After incubation for 30 min at 37 °C, 100 μl of DMEM medium containing 20% FBS was added and incubated for a further 16–48 h in a 5% CO_2 incubator. The formation of aggregates in the transfected cells was monitored using a fluorescence microscope. For the quantitation of intracellular aggregation, the culture medium was discarded by decantation and the cells were overlaid with PBS containing 0.1% Triton X-100 and 0.1 μg/ml DAPI (4′,6-diamidino-2-phenylindole) followed by gentle rotation for 30 min in the dark. The Triton X-100-insoluble punctate fluorescence images were photographed using a IX71 fluorescence microscope (Olympus, Tokyo, Japan) and analyzed using the image-processing program "Image J" with "Analyze Particle" menu (Schneider et al., 2012).

For inhibitor assay, cells were treated for 30 min in DMEM medium with respective compound before addition of α-Syn fibrils. After 30 min incubation with fibrils, 100 μl of DMEM medium containing respective inhibitor and 20% FBS was added.

The effect of in vitro digestion of α-Syn fibrils with cathepsin B

In vitro-prepared α-Syn fibrils (500 μg/ml) were digested with proteinase K (concentration range 48–3125 ng/ml in PBS) or cathepsin B (concentration range 16–1000 ng/ml in 25 mM MES pH 5.0/1 mM EDTA/1 mM DTT) at 37 °C for 60 min followed by heat inactivation of enzymes at 95 °C for 5 min. Digested fibrils were analyzed by assessment of intracellular aggregate formation and western blotting.

Knockdown of cathepsin expression by siRNA

SiRNA sequences targeting human CTSB were synthesized by Bex Co., Ltd (Tokyo, Japan). The siRNA sequences were: sense, 5′-GAGUUA UGUUUACCGAGGAtt-3′; anti-sense, 5′-UCCUCGGUAAACAUAACUCtt-3′ (Parreno et al., 2008).

The HEK293F/Syn-ECFP cells were transfected with siRNAs at a final concentration of 25 nM using RNAiMAX (Thermo Fisher Scientific, Invitrogen) according to the manufacturer's instructions. Forty-eight hours after transfection, cells were collected in trypsin for the intracellular aggregate forming assay. The efficiency of cathepsin gene knockdown was evaluated by assessing the enzyme activities of the cell lysate with the fluorogenic substrates Z-Arg-Arg-MCA and MOCAc-Gly-Lys-Pro-Ile-Leu-Phe-Phe-Arg-Leu-Lys(Dnp)-D-Arg-NH2, (Peptide Institute Inc.) according to the recommended procedure.

Knockdown of autophagy pathways by siRNAs

SiRNA sequences against human ATG5 and LAMP-2 genes have been described previously (Watanabe and Tanaka, 2011; Gonzalez-Polo et al., 2005). ATG5 gene knockdown was evaluated by suppression of LC3-II accumulation by 1 μM rapamycin (Wako Pure Chemical Industries Ltd) treatment for 6 h in the growth medium. LAMP-2 gene knockdown was by reduction of LAMP-2 protein content in the cell lysate by western blotting with anti-LAMP-2 antibody. We also confirmed reduction of both genes by quantitative PCR with appropriate primer sets: ATG5; 5′-TTGACGTTGGTAACTGACAAAGT-3′/5′-TGTGATGTTCCAAGGA AGAGC-3′ (Watanabe et al., 2012); and LAMP-2; 5′-TGGCAATGATAC TTGTCTGCTG-3′/5′-ACGGAGCCATTAACCAAATACAT-3′.

Immunocytochemistry

Cells were fixed with 2% paraformaldehyde (PFA) in cultured medium for 10 min at room temperature. The fixed cells were permeabilized with 0.1% Triton X-100 in PBS for 10 min, and blocked with 5% normal goat serum (NGS) in PBS for 30 min. Next, cells were incubated with primary antibody in blocking solution for 1–2 h. Then, the cells were washed with PBS, and further treated with secondary antibody. For double-staining, this staining procedure was repeated for each

antigen and the primary antibodies were detected by Alexa488- and Alexa594-conjugated antibodies (Thermo Fisher Scientific, Molecular Probes). These cells were washed with PBS followed by DAPI staining. They were then washed with milliQ water (Merck Millipore), and finally mounted with FluorSave (Merck Millipore). Images were acquired as a Z stack (20–30 z-sections, 0.3–0.5 μm apart, 1024 × 1024) through Plan-Apochromat 40×/1.30 or 63×/1.40 Oil DIC objective lenses (Carl Zeiss, Oberkochen, Germany) with an inverted laser-scanning confocal microscope, LSM510 (Carl Zeiss) (Watanabe and Tanaka, 2011).

Time-lapse imaging of aggregate formation

For time-lapse monitoring of the intracellular aggregation formation process, HEK293F/Syn-EGFP cells were transfected with α-Syn fibrils in collagen-coated 16-well chamber slides (Thermo Fisher Scientific, Nunc, #178599) and visualized under a fluorescent microscope IX71 (Olympus) equipped with a Stage Top incubator (TOKAI HIT, Shizuoka Japan). Images were captured using a 40× objective at 15-minute intervals.

Statistics

Data are expressed as the means ± standard errors. p values were calculated by one-way ANOVA followed by Tukey's post-hoc test.

Results

Establishment of an assay system to measure intracellular aggregate formation by α-Syn fibrils in cultured cells

To investigate the process underlying formation of intracellular LB-like aggregates, we established a HEK293F cell line stably expressing α-Syn fused to ECFP (HEK293F/Syn-ECFP cells). Under normal growth conditions, ECFP fluorescence was present uniformly in the cells and no aggregation was observed at all. When *in vitro*-prepared α-Syn fibrils (Luk et al., 2009) were introduced into the cells, a large condensed fluorescent signal began to appear 4 h after introduction. It was possible to observe in real-time the formation of aggregates in these cells. However, to quantify the accumulated fluorescent signals accurately was impossible because of fluorescence owing to non-participating α-Syn-ECFP in the cytoplasm. To overcome this limitation of quantification, we employed a simple washout process using 0.1% Triton X-100 (Sacino et al., 2013). Permeabilization of cell membranes allowed soluble α-Syn-ECFP to diffuse out of cells, but the detergent-resistant aggregates were retained (Fig. 1A). Varying amounts of *in vitro*-prepared α-Syn fibrils produced detergent-resistant fluorescent signals in HEK293F/Syn-ECFP cells, and a good correlation was obtained between the amounts of input α-Syn fibrils (Fig. 1B) and the number of particles (Fig. 1C), the total area (Fig. 1D), and the size of the signals (Fig. 1E). The insoluble α-Syn-ECFP aggregates were analyzed by conventional western blotting after separation of Triton X-100-insoluble protein by centrifugation (Supplementary Fig. S1). The levels of insoluble α-Syn-ECFP aggregates on the PVDF membranes appeared to increase in a dose-dependent manner with the amount of introduced α-Syn fibrils. However, it was considered that accurate quantification of aggregates on western blotting membranes was difficult because of the increase in the amounts of ladders and smeared bands derived from α-Syn-ECFP with a structure that is not separable on SDS-PAGE (Supplementary Fig. S1).

Monomeric α-Syn was polymerized by stirring *in vitro* to obtain fibril samples (Volpicelli-Daley et al., 2011), so that the process of aggregation could be monitored indirectly by an assay with fluorescent dye binding (Supplementary Fig. S2A) or sedimentation of the aggregates by ultracentrifugation (Supplementary Fig. S2B). When α-Syn monomer or *in vitro* samples have received <48 h of agitation were introduced into HEK293F/Syn-ECFP cells, no intracellular aggregate formation was observed (Supplementary Fig. S2C). However, when samples with a >96-h agitation period, which contained abundant fibrils (Supplementary Fig. S2B), were introduced into cells, intracellular

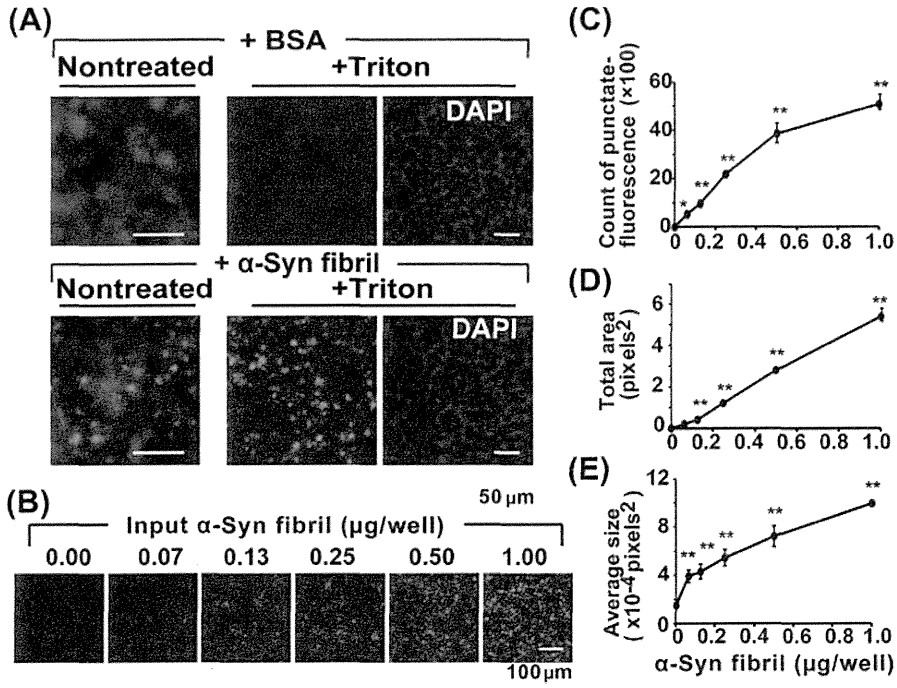

Fig. 1. Quantitative seeding activity assay for α-Syn aggregates. (A) Representative images of the intracellular aggregate quantification process are shown. After introduction of α-Syn fibrils into the Syn-ECFP-expressing cells (HEK293F/Syn-ECFP cells), cells started to form aggregates in the cytoplasm within a few hours (lower left panel). After washout of free Syn-ECFP with Triton X-100, only detergent-resistant α-Syn aggregates were retained in the cytoplasm (lower middle panel). DAPI staining was performed to confirm the presence of cells and to allow correction for cell number (right panels). (B) Aggregate formation was examined using varying amounts of α-Syn fibrils. (C–E) Then, fluorescent signals were analyzed using "Image J" and presented as graphs (*p < 0.05, **p < 0.01 from the no fibril control).

α-Syn-ECFP aggregates were observed as bright fluorescent signals and the number and size of aggregates increased with agitation time. We decided to use fibrils created by 168 h of stirring as seeds. Measuring the total area of aggregates is considered as an appropriate means of representing the seeding activity of fibril-containing samples. The introduction α-Syn fibrils and the fibril-induced formation of intracellular aggregates for 24 h were not toxic to the HEK293F/Syn-ECFP cells based on a lactate dehydrogenase (LDH) assay, excluding a possible influence of cell toxicity from this assay (Supplementary Fig. S2D).

Inhibition of lysosomal function suppresses α-Syn aggregate formation

To investigate the pathways mediating intracellular aggregate formation by α-Syn, we examined several inhibitors of the proteasome and ALP because disturbances of these degradation pathways are involved in protein aggregation (Ebrahimi-Fakhari et al., 2012). As shown in Figs. 2A and B, lactacystin, a proteasome inhibitor, had no effect on aggregate formation, but bafilomycin A1 and NH_4Cl, which neutralize lysosomal pH, strongly suppressed it in HEK293F/Syn-ECFP cells. This result suggested that lysosomal functions were involved in aggregate formation. Then, the effects of inhibitors of lysosomal enzymes on the degree of aggregate formation were examined. E-64d, an inhibitor of cysteine proteases, and CA-074Me, a cathepsin B-specific inhibitor, significantly blocked aggregate formation. Cathepsin B is a cysteine protease found abundantly in lysosomes. In contrast, pepstatin A, an inhibitor of aspartic proteases represented by cathepsin D, had no effect. In general, inhibition of the proteolytic process leads to accumulation of proteins destined for degradation. It was a surprise that the opposite result to what we anticipated was obtained from the cathepsin B inhibitor experiment. We introduced α-Syn fibrils and performed LDH assays using cathepsin B or cathepsin D inhibitor up to 72 h later. Following fibril introduction, LDH levels significantly increased at 48 h and 72 h, but not 24 h. However, toxicity was not different among groups treated with DMSO, Ca74Me, or pepstatin A (Supplementary Fig. S2E), and may be due to the long-term effects of fibril introduction.

We also investigated the role of endocytosis in aggregate formation using sertraline, an endocytosis inhibitor, to suppress dynamic GTPase activity (Takahashi et al., 2010). With sertraline, we observed marked inhibition of α-Syn aggregate formation (Fig. 2C), suggesting that exogenous α-Syn fibrils enter the cell and reach lysosomes *via* endocytosis.

In vitro digestion of α-Syn fibrils by cathepsin B enhances seeding activity

As shown in Fig. 2, cathepsin B may promote aggregate formation activity. Therefore, next, we examined whether the seeding activity was influenced by the extent of digestion of α-Syn fibrils by cathepsin B, with proteinase K digestion used as a control. Proteinase K preferentially digests proteins after hydrophobic amino acids; therefore, proteinase K induced almost complete digestion of α-Syn fibrils and intracellular aggregates were not formed (Figs. 3A and B, left). In contrast, cathepsin B digestion enhanced intracellular aggregate formation activity, which increased together with an increase in cathepsin B concentration (Figs. 3A and B, right). Cathepsin B preferentially cleaves -Arg-Arg-|-Xaa bonds in small molecule substrates (UniProt: P07858). However, human α-Syn does not have such sequences for cleavage. Thus, the levels of partially cathepsin B-digested fibrils and slightly truncated α-Syn were present at increased levels on SDS-PAGE gels (Fig. 3B, right, arrows a and b). Moreover the band indicated by arrow 'b' and shorter truncated bands were not recognized by the C20 antibody, which was raised against the C-terminal region of human α-Syn (Fig. 3D). This increase in aggregate-forming activity might be attributed to C-terminally truncated fibril seeds formed owing to the dipeptidyl carboxypeptidase activity of cathepsin B with broad substrate specificity (Koga et al., 1991).

Knockdown of the cathepsin B gene leads to decreased α-Syn aggregate formation

To examine the effect of cathepsin B gene (CTSB) suppression on α-Syn aggregate formation, the CTSB gene was knocked down by siRNA. As shown in Fig. 4A, the enzymatic activity of cathepsin B in the cell lysate was suppressed to 45% by the CTSB siRNA. Using cells with reduced cathepsin B activity, intracellular α-Syn aggregate formation was examined. About 40% suppression of seeding activity was observed in CTSB knocked down cells (Fig. 4B). Because cathepsin B was reported

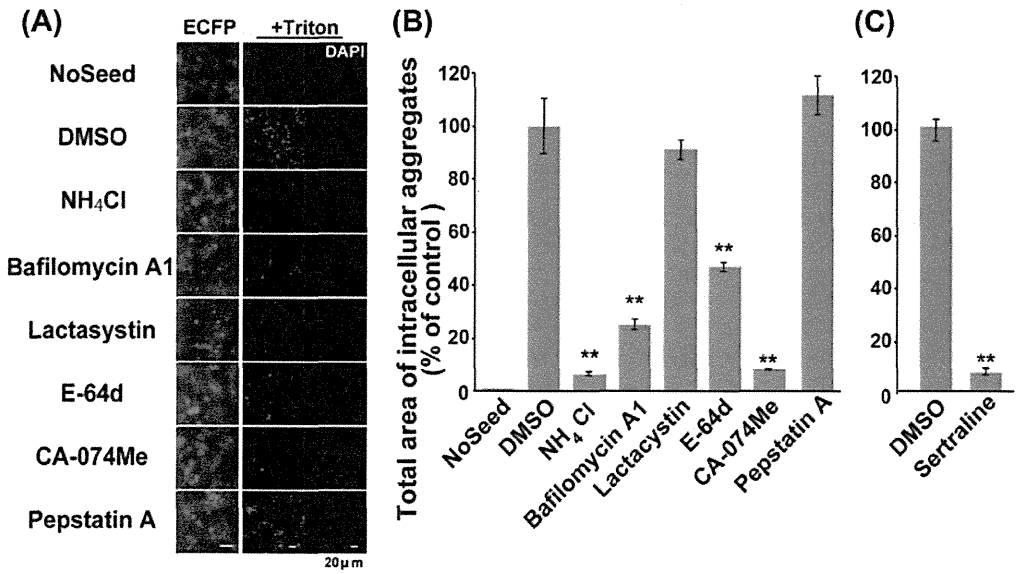

Fig. 2. Effect of inhibitors on intracellular aggregate formation. Various inhibitors that affect intracellular pH gradient and proteolysis were added during intracellular aggregate formation. (A) Representative fluorescence images of Triton X-100-resistant inclusions are shown in inhibitor-treated HEK293F/Syn-ECFP cells after α-Syn fibril introduction. Images of DAPI-stained cells are attached for the confirmation of the existence of the cells. Scale bar = 20 μm. (B) The effects of the reagents on aggregate formation are represented as the % of the level of aggregate formation in the DMSO control sample. The inhibitors used were 0.1% DMSO (0.1%) as a control, NH_4Cl (20 mM), bafilomycin A1 (10 nM), lactacystin (5 μM), CA-074Me (5 μM), E-64d (5 μM) and pepstatin A (5 μM). **$p < 0.01$ *vs.* the DMSO control. (C) The effect of endocytosis inhibitor sertralin (10 μM) is represented as (B).

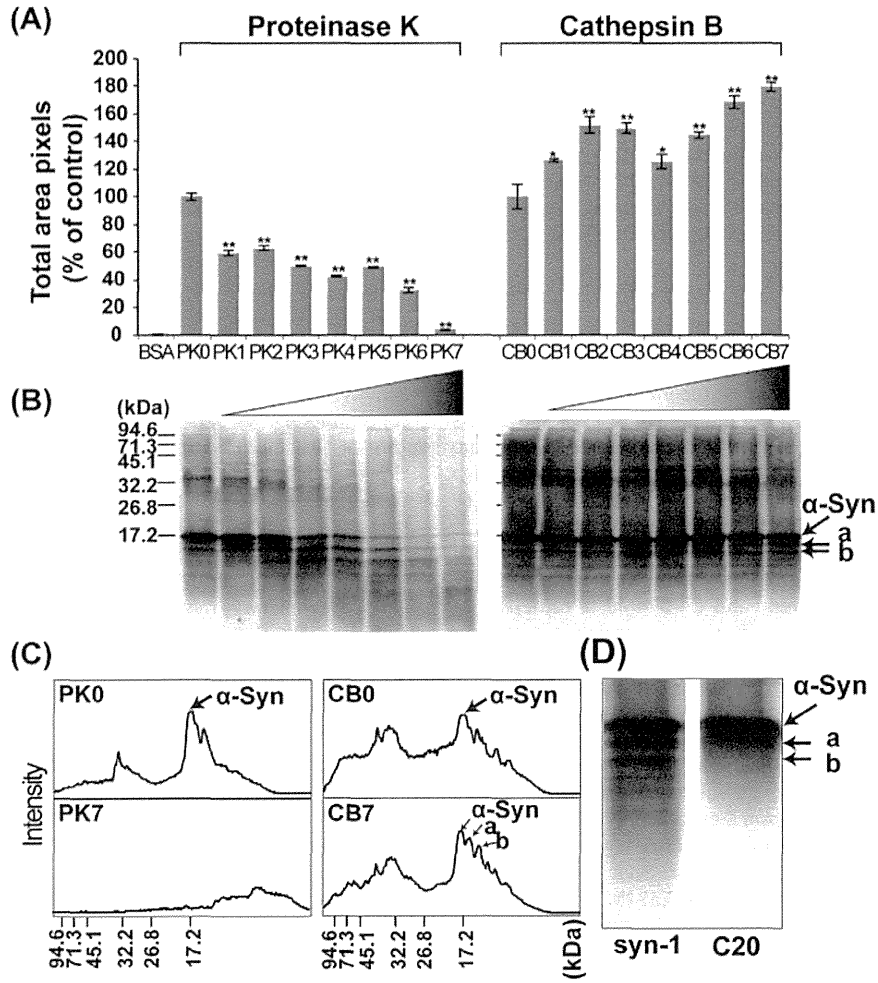

Fig. 3. *In vitro* cathepsin B digestion enhanced aggregate-forming activity. *In vitro*-prepared α-Syn fibrils were digested with proteinase K or cathepsin B at various enzyme concentrations. (A) The intracellular aggregate-forming activity was measured on the basis of protease-digested fibrils. The concentration of the enzyme increases from left to right (PK0 and CB0 represent no enzyme controls, PK1 to PK7 represent proteinase K concentrations from 48 ng/ml to 3125 ng/ml doubling each time, and CB1 to CB7 represent cathepsin B enzyme concentrations from 16 ng/ml to 1000 ng/ml doubling each time). $^{*}p < 0.05$, $^{**}p < 0.01$ *vs.* no enzyme control. (B) The degrees of cleavage by the enzymes were analyzed by western blotting using anti α-Syn monoclonal antibody (syn-1). Bands with distinguishable intensity changes associated with cathepsin B concentration were labeled with arrows "a" and "b". The molecular weights of monomeric α-Syn, and bands a and b on SDS-PAGE, correspond to 17.6, 16.4, and 14.9 kDa, respectively. (C) Profile plots for lanes PK0, PK7, CB0 and CB7 in (B) are shown. (D) Western blotting of the CB7 sample using syn-1 and C20 anti-α-Syn antibodies.

to be required for the activation of cathepsin D in lysosomes (Laurent-Matha et al., 2006), there was a possibility that the reduction of aggregate formation by CTSB knockdown was a result of the reduction in cathepsin D activity. However, as shown in Fig. 4A, the cathepsin D activity was not affected by CTSB knockdown, excluding the involvement of cathepsin D. Considering together the results of these experiments using specific inhibitors and siRNA, cathepsin B is considered to be responsible for the enhancement of α-Syn aggregate-forming activity.

Autophagy pathways are involved in α-Syn aggregate formation

In addition to endosome trafficking, autophagy pathways are known to be involved in intracellular protein transport to lysosomes (Saftig and Klumperman, 2009). Thus, we examined the contribution of autophagy by knockdown experiments using siRNA-ATG5 or siRNA-LAMP-2. Inhibition of macroautophagy by siRNA-ATG5 treatment led to a decrease in intracellular aggregate formation to 51% of control siRNA levels (Figs. 5A–C). Inhibition of chaperone-mediated autophagy (CMA) by siRNA-LAMP-2 also decreased aggregate formation to 61% of control levels, which was comparable to reductions in LAMP-2 gene and protein expression (Figs. 5D–F). These results indicate that both macroautophagy and CMA are involved in aggregate formation after incorporation of α-Syn fibrils.

Intracellular α-Syn aggregate formation begins in the lysosome

Because cathepsin B was involved in the aggregate formation by exogenous α-Syn fibrils in the above experiments, we next examined visually the location and growth of intracellular aggregates using the anti-pSyn antibody, which reportedly recognizes phosphorylated α-Syn at position serine 129 in synucleinopathy lesions (Fujiwara et al., 2002). As shown in Fig. 6A, exogenous α-Syn fibrils were surrounded by the lysosomal membrane marker LAMP-1 at 4 h after introduction of fibrils into the cells. It was considered that the seeding activity of the introduced fibrils was acquired in the lysosomes. Then, we examined the expression of newly formed aggregates after mutant α-Syn S129A fibril introduction. This time the anti-pSyn exclusively recognizes endogenous α-Syn. Intracellular aggregates appeared with small and weak phosphorylation signals within a few hours, and then gradually increased in number and size over time (Figs. 6B–D). Regarding the changes in size, the size-distributions of aggregates on confocal

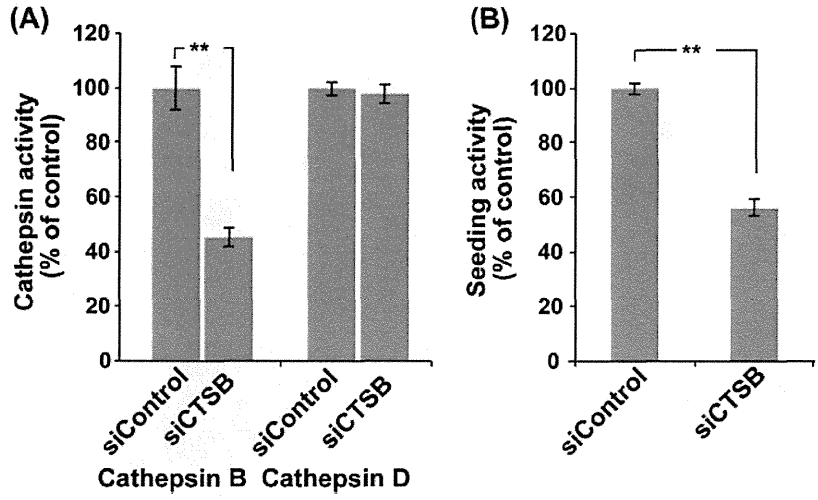

Fig. 4. Knockdown of the cathepsin B gene led to decreased aggregate-forming activity. (A) HEK293F/Syn-ECFP cells were transfected with an siRNA against the cathepsin B gene (CTSB) or a control siRNA for 2 days and cathepsin B and cathepsin D activities in the cell lysate were measured using fluorogenic substrates. The enzymatic activity of cathepsin B was decreased to 45% of the control level by the specific siRNA. The enzymatic activity of cathepsin D was not influenced by treatment with CTSB siRNA. (B) The intracellular seeding activity for aggregates formation was also measured after α-Syn fibril introduction. Similarly, seeding activity was also reduced to 56% of the control level after treatment with CTSB siRNA. Data are presented as the mean ± standard errors (**$p < 0.01$ from the control siRNA).

microscope images are presented in a histogram (Supplementary Fig. S3). Three hours after fibril introduction, approximately 70% of the intracellular aggregates were classified into the smallest fraction. As incubation time increased, the proportion of the smallest size fraction decreased, and the amount of larger aggregates increased (Supplementary Fig. S3). It was concluded that the intracellular aggregates begin as small aggregates, and grow larger within a day in this system.

Next, we examined the growth and localization of intracellular pSyn-positive aggregates with special reference to the coexistence with LAMP-1 (Fig. 6E). Intracellular aggregates showed one of three different forms: (a) they were completely included in the LAMP-1 signals; (b) they were partially surrounded by LAMP-1 signal; or (c) they existed independently from LAMP-1 signal. For example, compared with the aggregates shown in panel (a) of Fig. 6E, larger

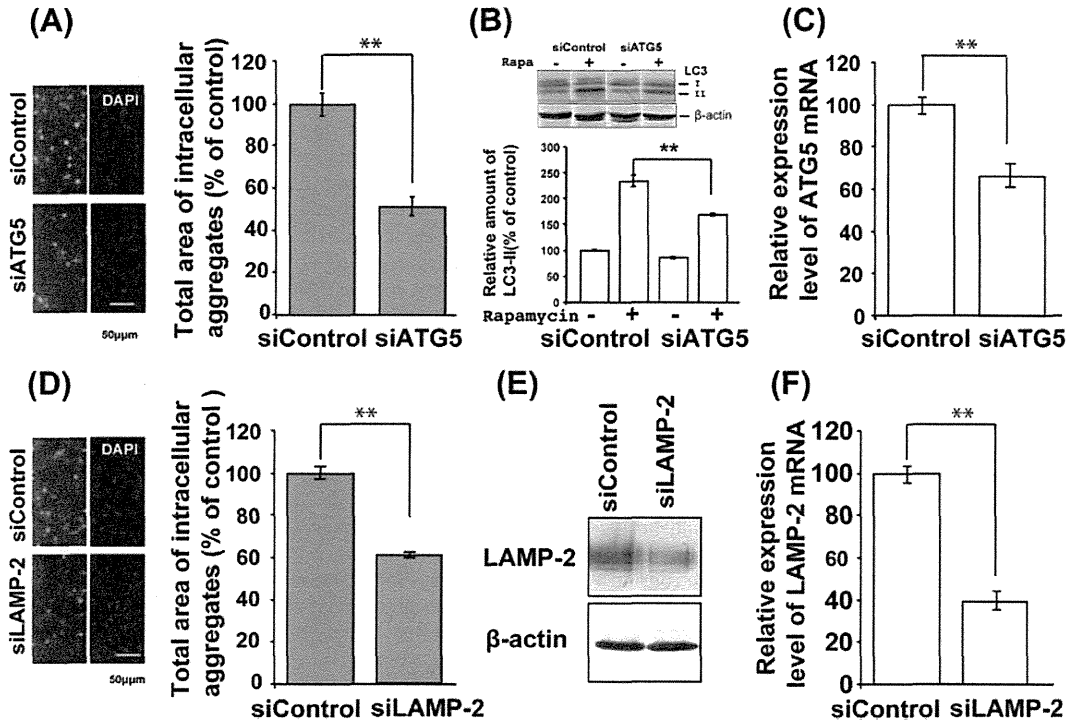

Fig. 5. Involvement of autophagy pathways in aggregate formation. Autophagy pathway component genes were knocked down using specific siRNAs. (A) Images of Triton X-100 resistant α-Syn aggregates and calculated total area of intracellular aggregates in siRNA treated cells were shown. ATG5 gene knockdown reduced aggregate formation to 51% of control levels. (B) Introduction of siATG5 suppressed rapamycine induced LC3-II accumulation analyzed by Western blotting with anti LC3 antibody. (C) ATG5 gene knockdown was confirmed by quantitative PCR. (D) LAMP-2 gene knockdown reduced fibril-induced aggregate formation to 61% of control levels. (E) Intracellular content of LAMP-2 protein in siRNA treated cells was decreased to 60%, as determined by western blotting. (F) Knockdown of LAMP-2 gene expression was determined by quantitative PCR. **$p < 0.01$ *vs.* siControl.

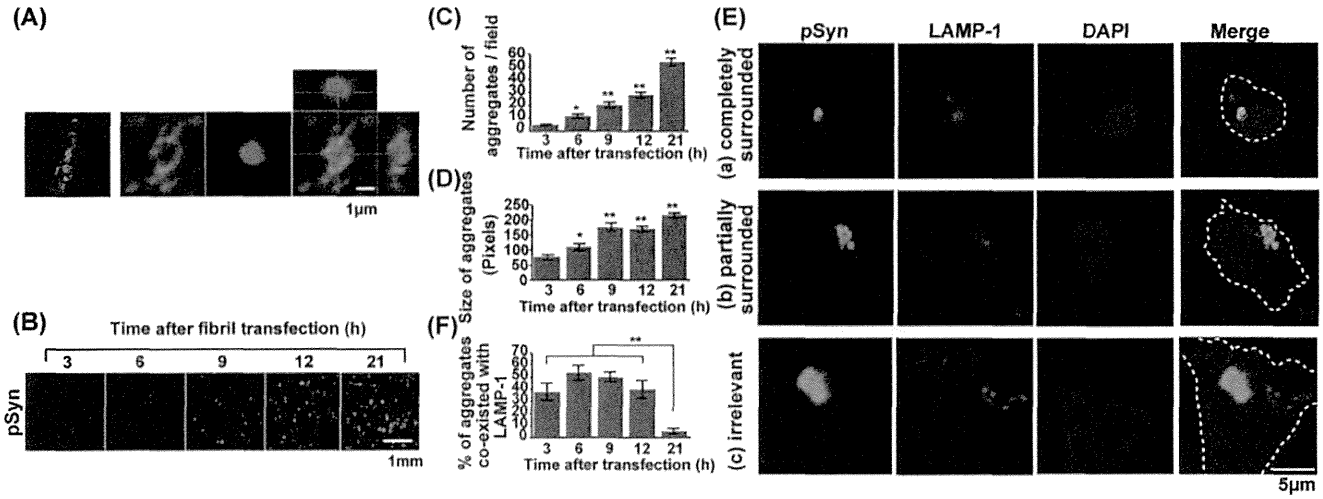

Fig. 6. Lysosomes as a location for intracellular aggregate formation. The location and development of newly generated aggregates were analyzed. (A) At 4 h after human α-Syn fibril introduction into HEK 293 cells, which do not express α-Syn, the intracellular location of exogenous α-Syn fibril was examined by double immunocytochemistry using antibodies against anti pSyn (red) and the lysosomal marker LAMP-1 (green). White dashed lines indicated the contours of the cells. White box areas were enlarged and merged images with x-z and y-z images were arranged. (B) Representative fluorescence images of the formation and the growth of intracellular aggregates along the time course after fibril introduction. Intracellular aggregates in HEK293F/Syn (without ECFP tag) cells, formation of which was initiated by *in vitro*-prepared S129A mutant fibrils, were stained with anti-pSyn antibody. (C), (D) The quantified time course-change of the number (C) and size (D) of intracellular aggregates on microscopic images of the same samples in (B). "Two hundred pixels" in (D) are equivalent to the area of a circle with a diameter of 5 μm in (B). (E) Confocal microscopic images of the three typical relationships of the intracellular aggregates to LAMP-1 staining are shown. White dashed lines in the panels indicate the contours of the cells. (F) Percentage of intracellular aggregates existing with LAMP-1 ((a) and (b) in panel (E) combined) are summarized. The data in (C), (D) and (F) are presented as the means ± standard errors (*$p < 0.05$, **$p < 0.01$ from the 3-h samples in (C) and (D), and from the 2-h sample in (F), respectively).

aggregates with irregular shapes were seen protruding from the lysosomal structure (panel (b)). Aggregates that coexisted with LAMP-1 (Figs. 6E-a and b) were counted at each time point examined after fibril introduction (Fig. 6F). The percentage of coexistence of pSyn aggregates and LAMP-1 showed a peak at 6 h, and then began decreasing. At 21 h, almost no aggregates coexisting with LAMP-1 were seen (Fig. 6F).

Live-cell imaging of growing α-Syn aggregates in cells

We also performed time-lapse imaging of intracellular aggregates forming in living HEK293F/Syn-EGFP cells (Supplementary Movies S1–3). In α-Syn-EGFP expressing cells, there were always dark regions lacking EGFP fluorescence in the cytoplasm (Figs. 7A, B). After 5 h of α-Syn fibril introduction, small aggregates that appeared brighter than the cytoplasm began to appear in the dark compartments. These gradually grew larger and filled the dark places with aggregates (Figs. 7A a–c, Supplementary Movies S1–3). The cells in which aggregations grew to a large size tended to rapidly consume endogenous Syn-EGFP molecules for aggregate formation resulting in a reduction in cytoplasmic fluorescence (Figs. 7Ac). Next, we stained these dark compartments with LysoTracker or LAMP-1 antibody (at 6 h after α-Syn fibril introduction). While cytoplasmic dark compartments in HEK293F/Syn-EGFP cells were not stained with LysoTracker (white arrow heads in Fig. 7B upper panels), most of them were LAMP-1-positive (white arrows in Fig. 7B lower panels). The LysoTracker probes are used to detect acidic organelles in living cells and normal lysosomes are usually positive for both LysoTracker and LAMP-1 (Supplementary Fig. S4). These LAMP-1-positive/LysoTracker-negative dark compartments are considered to be impaired lysosomes. Based on these observations, it is strongly suggested that the initiation of aggregate formation takes place in the lysosomes after α-Syn fibril treatment, and the growth of aggregates is followed by their escape from the impaired lysosomes.

Discussion

Although several groups have reported the formation of LB-like aggregates in cells by exogenous α-Syn fibrils, how they grow into larger molecules involving endogenous α-Syn is still unknown (Luk et al., 2009; Nonaka et al., 2010; Watanabe et al., 2012; Tanik et al., 2013). To address this issue, we developed an assay system for forming detergent-insoluble α-Syn aggregates using HEK293 cells stably expressing α-Syn-ECFP. This system easily enabled the quantification of the fluorescence intensity of α-Syn-containing intracellular aggregates and quantification of the number and size of aggregates. Recently Guo et al reported that there are at least two conformational variations of sarkosyl-insoluble α-Syn in PD brains (Guo et al., 2013). Thus, in addition to assessing *in vitro*-prepared fibrils, the present assay system could be useful for examining pathological features in synucleinopathy patients and classifying the precise type of α-Syn pathology.

We previously observed that intracellular α-Syn inclusions, formation of which was induced by exogenous α-Syn fibrils, underwent degradation *via* p62/SQSTM1-dependent autophagy in HEK293 cells (Watanabe et al., 2012). Therefore, at first, we thought that inhibition of the degradation pathway would be involved in the formation of aggregates, and we treated cells with inhibitors of the ALP or the ubiquitin–proteasome system. Unexpectedly, treatment with bafilomycin A1, which blocks vacuolar H^+-ATPase (V-ATPase) and prevents fusion between autophagosomes and mature lysosomes (Yamamoto et al., 1998), decreased aggregate formation, while the proteasome inhibitor lactacystin did not affect aggregate formation. Klucken et al also reported this bafilomycin A1-induced inhibition of aggregation using α-Syn-transfected H4 cells, which were prone to development of α-Syn aggregates (Klucken et al., 2012). They also showed that another V-ATPase inhibitor, chloroquine, substantially reduced aggregation, but that 3-methyladenine, which inhibits autophagy by blocking autophagosome formation, did not. Moreover, NH_4Cl treatment, which blocks acidification, reduced aggregate formation in this study. Recently, Buell et al. reported that, in the presence of preformed fibrils, the multiplication of aggregates was much faster at lower pH values below 6 than at normal physiological pH values *in vitro* (Buell et al., 2014). These lines of evidence suggest that lysosomal function is important for initiating aggregation from the seed of α-Syn fibrils.

It is generally thought that lysosomal impairment causes α-Syn accumulation (Dehay et al., 2013). In fact, concerning another abundant lysosomal enzyme, cathepsin D, there were reports that a deficiency of cathepsin D or overexpression of an inactive mutant cathepsin D caused

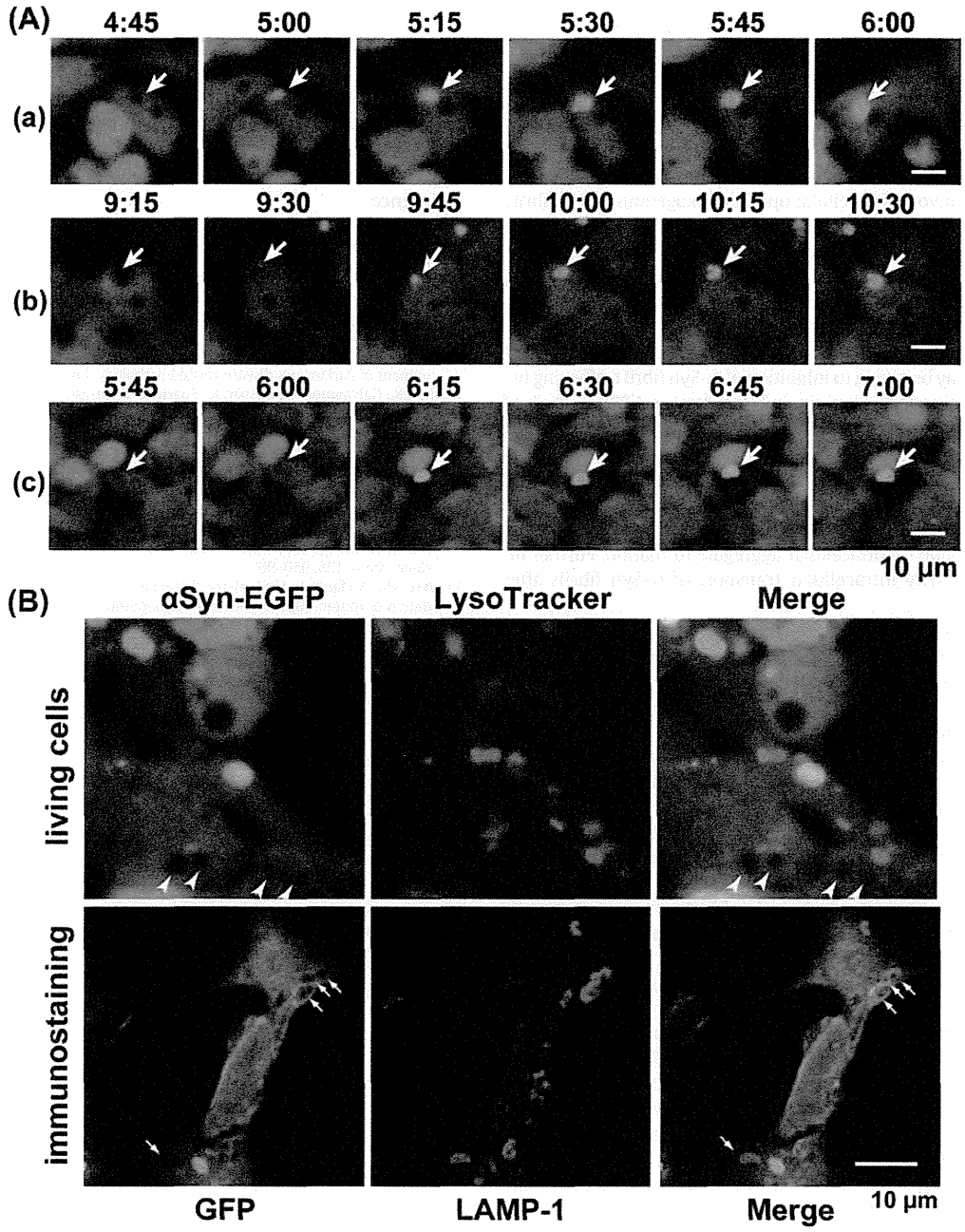

Fig. 7. α-Syn aggregates emerge from dysfunctional lysosomes. (A) Three representative time-lapse image sequences of intracellular α-Syn aggregate formation are shown. Time after fibril transfection into HEK293F/syn-EGFP cells is shown as h:mm above the images. White arrows indicate the positions of arising α-Syn intracellular aggregates. (B) Upper panels show the fluorescence images of living HEK293/syn-EGFP cells, which were stained with LysoTracker Red at 6 h after α-Syn fibril introduction. Lower panels show the immunocytochemistry of fibril-transfected HEK293/syn-EGFP cells using anti-GFP and anti-LAMP-1 antibodies. Arrowheads indicate the cytoplasmic dark compartments that exclude EGFP fluorescence and LysoTracker signals, and arrows indicate those stained with LAMP-1 signals.

accumulation of α-Syn and toxicity (Qiao et al., 2008; Cullen et al., 2009; Crabtree et al., 2014). In the present study, we observed that cathepsin D inhibitor had no effect on aggregate formation. There may not have been enough time to enhance endogenous α-Syn expression and aggregate formation in this assay system. Thus, our present study revealed that, among lysosomal enzymes, cathepsin B is responsible for the activation of α-Syn seeds. This may be attributed to the fact that α-Syn does not have a typical consensus recognition sequence for cathepsin B. α-Syn fibrils pre-treated with cathepsin B *in vitro* were not completely digested and slightly truncated forms appeared after digestion in a high enzyme concentration on western blots. This pre-treatment with high doses of cathepsin B caused more aggregate formation in cells (Fig. 3). In the case of C-terminal truncated α-Syn, it enhances the aggregation of the more abundant full-length α-Syn *in vitro* and *in vivo* (Murray et al., 2003; Li et al., 2005; Ulusoy et al., 2010). In fact, LB extracts contain up to 15% C-terminal truncated α-Syn (Baba et al., 1998). Transgenic mice with truncated human α-Syn (1-120), driven by the tyrosine hydroxylase promoter, show pathological inclusions in the substantia nigra and olfactory bulb (Tofaris et al., 2006). Furthermore, Games et al. recently reported that reducing C-terminal truncated α-Syn by passive immunization in mThy1-α-Syn transgenic mice, attenuated neurodegeneration (Games et al., 2014).

These reports suggest that C-terminal truncated α-Syn plays an important role in pathogenesis of synucleinopathies. In this study, cathepsin B-induced partially cleaved and/or conformationally changed α-Syn fibrils are supposed to gain nucleation activity and induce formation of intracellular aggregates of α-Syn. The precise mechanism underlying the modulation of α-Syn fibrils by cathepsin B will be clarified in a future study.

Endocytosis is involved in cellular uptake of exogenous α-Syn fibrils. Our findings suggest that after endocytosis, macroautophagy plays a part in transport of α-Syn fibrils to lysosomes. We previously showed that exogenous fibrils colocalized with LC3 1 h after introduction into HEK 293 cells. As there is no endogenous α-Syn, exogenous fibrils underwent further degradation through the ALP (Watanabe et al., 2012). In the present study, suppression of α-Syn aggregate formation by siRNA-ATG5 may be owing to inhibition of α-Syn fibril trafficking before the fibrils attain seeding activity in lysosomes, as ATG5 is involved in elongation of isolated membranes in autophagosome formation (Kuma et al., 2004). On the other hand, CMA reportedly contributes to α-Syn monomer transfer to lysosomes and subsequent degradation (Cuervo et al., 2004; Xilouri et al., 2009). SiRNA-LAMP-2 treatment may inhibit transport of endogenous α-Syn monomers into lysosomes and prevent initiation of intracellular aggregate formation. Further investigation will clarify intracellular transport of α-Syn fibrils after transfection.

We observed that aggregate formation begins in the lysosome. From 4 h after fibril introduction, small aggregates including endogenous phosphorylated α-Syn appeared. At first, they were surrounded by a lysosomal marker, LAMP-1 (Figs. 6E-a). Endogenous soluble α-Syn is recruited to exogenous α-Syn fibrils and is converted into insoluble, hyperphosphorylated, and ubiquitinated pathological species in cultured cells (Luk et al., 2009). Enhanced or overexpressed neuronal α-Syn is degraded in the lysosome *via* CMA *in vivo* (Mak et al., 2010). Thus, the lysosome seems to provide a place of aggregation from fibril seeds in the early period after introduction. Our present data showed that more than 90% of α-Syn aggregates were not colocalized with LAMP-1 at 21 h after fibril introduction (Fig. 6F). Freeman et al recently reported that *in vitro*-prepared α-Syn aggregates could induce rupture of the lysosome following their endocytosis after 24 h in neuronal cell lines (Freeman et al., 2013). Using an HEK293 model of LB-like aggregates, Tanik et al reported that the amounts of giant lysosomes increased 24 h after introduction of preformed fibrils and, at that time, α-Syn aggregates were not colocalized with LAMP-1 (Tanik et al., 2013). Collectively, based on these results and our own, we propose a model in which α-Syn seeds are initially activated in the lysosome by cathepsin B, rapidly grow larger and incorporate endogenous α-Syn, and escape from the lysosome 24 h after introduction.

Recently it was reported that LB-like aggregates are spread in the brain by inoculating α-Syn fibrils (Luk et al., 2012a,b; Masuda-Suzukake et al., 2013). Precise knowledge about the process underlying intracellular α-Syn aggregation after seeding with fibrils will contribute to new therapeutic strategies for PD and DLB in the future.

Supplementary data to this article can be found online at http://dx.doi.org/10.1016/j.nbd.2014.10.011.

Conflict of interest

The authors declare no conflict of interest.

Acknowledgments

The anti-LAMP-1 antibody developed by J. Thomas August and James E. K. Hildreth was obtained from the Developmental Studies Hybridoma Bank, developed under the auspices of NICHD, National Institutes of Health, and maintained by the Department of Biology, University of Iowa.

This work was supported in part by Grants-in-Aid for Scientific Research from the Japan Society for Promotion of Science (YW: 24591272 and MT: 25290014) and a grant from the Adaptable and Seamless Technology Transfer Program through Target-driven R&D from the Japan Science and Technology Agency (MT: AS242Z01075Q).

References

Alvarez-Erviti, L., Seow, Y., Schapira, A.H., Gardiner, C., Sargent, I.L., Wood, M.J., Cooper, J.M., 2011. Lysosomal dysfunction increases exosome-mediated alpha-synuclein release and transmission. Neurobiol. Dis. 42, 360–367.

Baba, M., Nakajo, S., Tu, P.H., Tomita, T., Nakaya, K., Lee, V.M., Trojanowski, J.Q., Iwatsubo, T., 1998. Aggregation of alpha-synuclein in Lewy bodies of sporadic Parkinson's disease and dementia with Lewy bodies. Am. J. Pathol. 152, 879–884.

Braak, H., Ghebremedhin, E., Rub, U., Bratzke, H., Del Tredici, K., 2004. Stages in the development of Parkinson's disease-related pathology. Cell Tissue Res. 318, 121–134.

Buell, A.K., Galvagnion, C., Gaspar, R., Sparr, E., Vendruscolo, M., Knowles, T.P., Linse, S., Dobson, C.M., 2014. Solution conditions determine the relative importance of nucleation and growth processes in alpha-synuclein aggregation. Proc. Natl. Acad. Sci. U. S. A. 111, 7671–7676.

Conway, K.A., Harper, J.D., Lansbury, P.T., 1998. Accelerated in vitro fibril formation by a mutant α-synuclein linked to early-onset Parkinson disease. Nat. Med. 4, 1318–1320.

Crabtree, D., Dodson, M., Ouyang, X., Boyer-Guittaut, M., Liang, Q., Ballestas, M.E., Fineberg, N., Zhang, J., 2014. Over-expression of an inactive mutant cathepsin D increases endogenous alpha-synuclein and cathepsin B activity in SH-SY5Y cells. J. Neurochem. 128, 950–961.

Cuervo, A.M., Stefanis, L., Fredenburg, R., Lansbury, P.T., Sulzer, D., 2004. Impaired degradation of mutant alpha-synuclein by chaperone-mediated autophagy. Science 305, 1292–1295.

Cullen, V., Lindfors, M., Ng, J., Paetau, A., Swinton, E., Kolodziej, P., Boston, H., Saftig, P., Woulfe, J., Feany, M.B., Myllykangas, L., Schlossmacher, M.G., Tyynela, J., 2009. Cathepsin D expression level affects alpha-synuclein processing, aggregation, and toxicity in vivo. Mol. Brain 2, 5.

Danzer, K.M., Kranich, L.R., Ruf, W.P., Cagsal-Getkin, O., Winslow, A.R., Zhu, L., Vanderburg, C.R., McLean, P.J., 2012. Exosomal cell-to-cell transmission of alpha synuclein oligomers. Mol. Neurodegener. 7, 42.

Dehay, B., Martinez-Vicente, M., Caldwell, G.A., Caldwell, K.A., Yue, Z., Cookson, M.R., Klein, C., Vila, M., Bezard, E., 2013. Lysosomal impairment in Parkinson's disease. Mov. Disord. 28, 725–732.

Desplats, P., Lee, H.J., Bae, E.J., Patrick, C., Rockenstein, E., Crews, L., Spencer, B., Masliah, E., Lee, S.J., 2009. Inclusion formation and neuronal cell death through neuron-to-neuron transmission of α-synuclein. Proc. Natl. Acad. Sci. U. S. A. 106, 13010–13015.

Ebrahimi-Fakhari, D., McLean, P.J., Unni, V.K., 2012. Alpha-synuclein's degradation in vivo: opening a new (cranial) window on the roles of degradation pathways in Parkinson disease. Autophagy 8, 281–283.

Emmanouilidou, E., Melachroinou, K., Roumeliotis, T., Garbis, S.D., Ntzouni, M., Margaritis, L.H., Stefanis, L., Vekrellis, K., 2010. Cell-produced α-synuclein is secreted in a calcium-dependent manner by exosomes and impacts neuronal survival. J. Neurosci. 30, 6838–6851.

Freeman, D., Cedillos, R., Choyke, S., Lukic, Z., McGuire, K., Marvin, S., Burrage, A.M., Sudholt, S., Rana, A., O'Connor, C., Wiethoff, C.M., Campbell, E.M., 2013. Alpha-synuclein induces lysosomal rupture and cathepsin dependent reactive oxygen species following endocytosis. PLoS ONE 8, e62143.

Fujiwara, H., Hasegawa, M., Dohmae, N., Kawashima, A., Masliah, E., Goldberg, M.S., Shen, J., Takio, K., Iwatsubo, T., 2002. Alpha-synuclein is phosphorylated in synucleinopathy lesions. Nat. Cell Biol. 4, 160–164.

Games, D., Valera, E., Spencer, B., Rockenstein, E., Mante, M., Adame, A., Patrick, C., Ubhi, K. , Nuber, S., Sacayon, P., Zago, W., Seubert, P., Barbour, R., Schenk, D., Masliah, E., 2014. Reducing C-terminal-truncated alpha-synuclein by immunotherapy attenuates neurodegeneration and propagation in Parkinson's disease-like models. J. Neurosci. 34, 9441–9454.

Giasson, B.I., Uryu, K., Trojanowski, J.Q., Lee, V.M., 1999. Mutant and wild type human α-synucleins assemble into elongated filaments with distinct morphologies in vitro. J. Biol. Chem. 274, 7619–7622.

Gonzalez-Polo, R.A., Boya, P., Pauleau, A.L., Jalil, A., Larochette, N., Souquere, S., Eskelinen, E.L., Pierron, G., Saftig, P., Kroemer, G., 2005. The apoptosis/autophagy paradox: autophagic vacuolization before apoptotic death. J. Cell Sci. 118, 3091–3102.

Guo, J.L., Covell, D.J., Daniels, J.P., Iba, M., Stieber, A., Zhang, B., Riddle, D.M., Kwong, L.K., Xu, Y., Trojanowski, J.Q., Lee, V.M., 2013. Distinct α-synuclein strains differentially promote tau inclusions in neurons. Cell 154, 103–117.

Hashimoto, M., Hsu, L.J., Sisk, A., Xia, Y., Takeda, A., Sundsmo, M., Masliah, E., 1998. Human recombinant NACP/α-synuclein is aggregated and fibrillated in vitro: relevance for Lewy body disease. Brain Res. 799, 301–306.

Klucken, J., Poehler, A.M., Ebrahimi-Fakhari, D., Schneider, J., Nuber, S., Rockenstein, E., Schlotzer-Schrehardt, U., Hyman, B.T., McLean, P.J., Masliah, E., Winkler, J., 2012. Alpha-synuclein aggregation involves a bafilomycin A 1-sensitive autophagy pathway. Autophagy 8, 754–766.

Koga, H., Yamada, H., Nishimura, Y., Kato, K., Imoto, T., 1991. Multiple proteolytic action of rat liver cathepsin B: specificities and pH-dependences of the endo- and exopeptidase activities. J. Biochem. 110, 179–188.

Kuma, A., Hatano, M., Matsui, M., Yamamoto, A., Nakaya, H., Yoshimori, T., Ohsumi, Y., Tokuhisa, T., Mizushima, N., 2004. The role of autophagy during the early neonatal starvation period. Nature 432, 1032–1036.

Laurent-Matha, V., Derocq, D., Prebois, C., Katunuma, N., Liaudet-Coopman, E., 2006. Processing of human cathepsin D is independent of its catalytic function and autoactivation: involvement of cathepsins L and B. J. Biochem. 139, 363–371.
Lee, H.J., Patel, S., Lee, S.J., 2005. Intravesicular localization and exocytosis of α-synuclein and its aggregates. J. Neurosci. 25, 6016–6024.
Li, W., West, N., Colla, E., Pletnikova, O., Troncoso, J.C., Marsh, L., Dawson, T.M., Jakala, P., Hartmann, T., Price, D.L., Lee, M.K., 2005. Aggregation promoting C-terminal truncation of alpha-synuclein is a normal cellular process and is enhanced by the familial Parkinson's disease-linked mutations. Proc. Natl. Acad. Sci. U. S. A. 102, 2162–2167.
Luk, K.C., Kehm, V., Carroll, J., Zhang, B., O'Brien, P., Trojanowski, J.Q., Lee, V.M., 2012a. Pathological α-synuclein transmission initiates Parkinson-like neurodegeneration in nontransgenic mice. Science 338, 949–953.
Luk, K.C., Kehm, V.M., Zhang, B., O'Brien, P., Trojanowski, J.Q., Lee, V.M., 2012b. Intracerebral inoculation of pathological α-synuclein initiates a rapidly progressive neurodegenerative alpha-synucleinopathy in mice. J. Exp. Med. 209, 975–986.
Luk, K.C., Song, C., O'Brien, P., Stieber, A., Branch, J.R., Brunden, K.R., Trojanowski, J.Q., Lee, V.M., 2009. Exogenous α-synuclein fibrils seed the formation of Lewy body-like intracellular inclusions in cultured cells. Proc. Natl. Acad. Sci. U. S. A. 106, 20051–20056.
Mak, S.K., McCormack, A.L., Manning-Bog, A.B., Cuervo, A.M., Di Monte, D.A., 2010. Lysosomal degradation of α-synuclein in vivo. J. Biol. Chem. 285, 13621–13629.
Marques, O., Outeiro, T.F., 2012. Alpha-synuclein: from secretion to dysfunction and death. Cell Death Dis. 3, e350.
Masuda-Suzukake, M., Nonaka, T., Hosokawa, M., Oikawa, T., Arai, T., Akiyama, H., Mann, D.M., Hasegawa, M., 2013. Prion-like spreading of pathological α-synuclein in brain. Brain 136, 1128–1138.
Murray, I.V., Giasson, B.I., Quinn, S.M., Koppaka, V., Axelsen, P.H., Ischiropoulos, H., Trojanowski, J.Q., Lee, V.M., 2003. Role of alpha-synuclein carboxy-terminus on fibril formation in vitro. Biochemistry 42, 8530–8540.
Nonaka, T., Watanabe, S.T., Iwatsubo, T., Hasegawa, M., 2010. Seeded aggregation and toxicity of α-synuclein and tau: cellular models of neurodegenerative diseases. J. Biol. Chem. 285, 34885–34898.
Parreno, M., Casanova, I., Cespedes, M.V., Vaque, J.P., Pavon, M.A., Leon, J., Mangues, R., 2008. Bobel-24 and derivatives induce caspase-independent death in pancreatic cancer regardless of apoptotic resistance. Cancer Res. 68, 6313–6323.
Protter, D., Lang, C., Cooper, A.A., 2012. αSynuclein and mitochondrial dysfunction: a pathogenic partnership in Parkinson's disease? Park. Dis. 2012, 829207.
Qiao, L., Hamamichi, S., Caldwell, K.A., Caldwell, G.A., Yacoubian, T.A., Wilson, S., Xie, Z.L., Speake, L.D., Parks, R., Crabtree, D., Liang, Q., Crimmins, S., Schneider, L., Uchiyama, Y., Iwatsubo, T., Zhou, Y., Peng, L., Lu, Y., Standaert, D.G., Walls, K.C., Shacka, J.J., Roth, K.A., Zhang, J., 2008. Lysosomal enzyme cathepsin D protects against alpha-synuclein aggregation and toxicity. Mol. Brain 1, 17.
Sacino, A.N., Thomas, M.A., Ceballos-Diaz, C., Cruz, P.E., Rosario, A.M., Lewis, J., Giasson, B.I., Golde, T.E., 2013. Conformational templating of α-synuclein aggregates in neuronal–glial cultures. Mol. Neurodegener. 8, 17.
Saftig, P., Klumperman, J., 2009. Lysosome biogenesis and lysosomal membrane proteins: trafficking meets function. Nat. Rev. Mol. Cell Biol. 10, 623–635.
Schneider, C.A., Rasband, W.S., Eliceiri, K.W., 2012. NIH Image to ImageJ: 25 years of image analysis. Nat. Methods 9, 671–675.
Sung, J.Y., Kim, J., Paik, S.R., Park, J.H., Ahn, Y.S., Chung, K.C., 2001. Induction of neuronal cell death by Rab5A-dependent endocytosis of α-synuclein. J. Biol. Chem. 276, 27441–27448.
Taguchi, K., Watanabe, Y., Tsujimura, A., Tatebe, H., Miyata, S., Tokuda, T., Mizuno, T., Tanaka, M., 2014. Differential expression of alpha-synuclein in hippocampal neurons. PLoS ONE 9, e89327.
Takahashi, K., Miyoshi, H., Otomo, M., Osada, K., Yamaguchi, N., Nakashima, H., 2010. Suppression of dynamin GTPase activity by sertraline leads to inhibition of dynamin-dependent endocytosis. Biochem. Biophys. Res. Commun. 391, 382–387.
Tanik, S.A., Schultheiss, C.E., Volpicelli-Daley, L.A., Brunden, K.R., Lee, V.M., 2013. Lewy body-like α-synuclein aggregates resist degradation and impair macroautophagy. J. Biol. Chem. 288, 15194–15210.
Tofaris, G.K., Garcia Reitbock, P., Humby, T., Lambourne, S.L., O'Connell, M., Ghetti, B., Gossage, H., Emson, P.C., Wilkinson, L.S., Goedert, M., Spillantini, M.G., 2006. Pathological changes in dopaminergic nerve cells of the substantia nigra and olfactory bulb in mice transgenic for truncated human alpha-synuclein(1–120): implications for Lewy body disorders. J. Neurosci. 26, 3942–3950.
Ulusoy, A., Febbraro, F., Jensen, P.H., Kirik, D., Romero-Ramos, M., 2010. Co-expression of C-terminal truncated alpha-synuclein enhances full-length alpha-synuclein-induced pathology. Eur. J. Neurosci. 32, 409–422.
Volpicelli-Daley, L.A., Luk, K.C., Patel, T.P., Tanik, S.A., Riddle, D.M., Stieber, A., Meaney, D.F., Trojanowski, J.Q., Lee, V.M., 2011. Exogenous α-synuclein fibrils induce Lewy body pathology leading to synaptic dysfunction and neuron death. Neuron 72, 57–71.
Watanabe, Y., Tanaka, M., 2011. p62/SQSTM1 in autophagic clearance of a non-ubiquitylated substrate. J. Cell Sci. 124, 2692–2701.
Watanabe, Y., Tatebe, H., Taguchi, K., Endo, Y., Tokuda, T., Mizuno, T., Nakagawa, M., Tanaka, M., 2012. p62/SQSTM1-dependent autophagy of Lewy body-like α-synuclein inclusions. PLoS ONE 7, e52868.
Xilouri, M., Brekk, O.R., Stefanis, L., 2013. α-Synuclein and protein degradation systems: a reciprocal relationship. Mol. Neurobiol. 47, 537–551.
Xilouri, M., Vogiatzi, T., Vekrellis, K., Park, D., Stefanis, L., 2009. Abberant α-synuclein confers toxicity to neurons in part through inhibition of chaperone-mediated autophagy. PLoS ONE 4, e5515.
Yamamoto, A., Tagawa, Y., Yoshimori, T., Moriyama, Y., Masaki, R., Tashiro, Y., 1998. Bafilomycin A1 prevents maturation of autophagic vacuoles by inhibiting fusion between autophagosomes and lysosomes in rat hepatoma cell line, H-4-II-E cells. Cell Struct. Funct. 23, 33–42.